Article:
Dan, A, Aery, S, Zhang, S et al. (3 more authors) (2020) Protein Microgel-Stabilized Pickering Liquid Crystal Emulsions Undergo Analyte-Triggered Configurational Transition. Langmuir, 36 (34). acs.langmuir.0c01345. pp. 10091-10102. ISSN 0743-7463

https://doi.org/10.1021/acs.langmuir.0c01345

Protein Microgel-Stabilized Pickering Liquid Crystal Emulsions Undergo Analyte-Triggered Configurational Transition

Abhijit Dan,*[†] Shikha Aery,[†] Shuning Zhang,[‡] Daniel Baker,[$] Helen F. Gleeson,[$] Anwesha Sarkar*[‡]

[†]Department of Chemistry and Centre for Advanced Studies in Chemistry, Panjab University − Chandigarh, Sector 14, Chandigarh, 160014, India

[‡]Food Colloids and Bioprocessing Group, School of Food Science and Nutrition, University of Leeds, LS2 9JT, UK.

[$]Soft Matter Physics Group, School of Physics and Astronomy, University of Leeds, LS2 9JT, UK.

Table of Content (TOC)

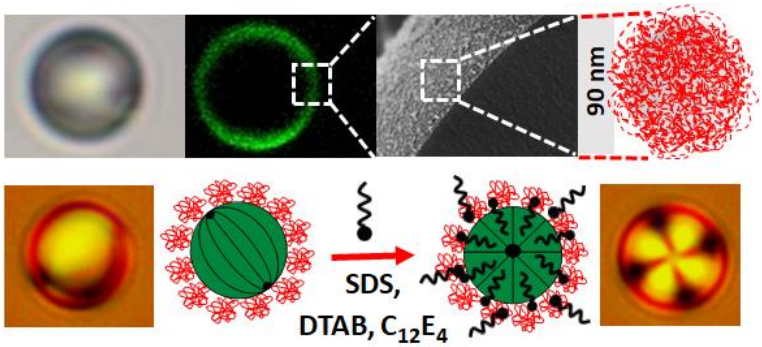

ABSTRACT

Herein, we report a novel approach that involves Pickering stabilization of micometer-sized liquid crystal (LC) droplets with biocompatible soft materials such as whey protein microgel (WPM) to facilitate the analysis of analyte-induced configurational transition of the LC droplets. The WPM particles were able to irreversibly adsorb at the LC-water interface and the resulting WPM-stabilized LC droplets possessed a remarkable stability against coalescence over time. Although the LC droplets were successfully protected by a continuous network of WPM layer, the LC-water interface was still accessible for small molecules such as sodium dodecyl sulphate (SDS) that could diffuse through the meshes of the adsorbed WPM network or through the interfacial pores and induce a LC response. This approach was exploited to investigate the dynamic range of the WPM-stabilized LC droplets response to SDS. Nevertheless, the presence of unadsorbed WPM in aqueous medium reduced the access of SDS molecules to the LC droplets, thus suppressing the configuration transition. An improved LC response to SDS with a lower detection limit was achieved after washing off the unadsorbed WPM. Interestingly, the LC exhibited a detection limit as low as ~0.85 mM for SDS within the initial WPM concentration ranging from 0.005 to 0.1 wt %. Further, we demonstrate that the dose-response behaviour was strongly influenced by the number of droplets exposed to the aqueous analytes as well as the type of surfactants such as anionic SDS, cationic dodecyltrimethylammonium bromide (DTAB) and non-ionic tetra(ethylene glycol)monododecyl ether ($C_{12}E_4$). Thus, our results address key issues associated with the quantification of aqueous analytes and provide a promising colloidal platform towards the development of new classes of biocompatible LC droplet-based optical sensors.

INTRODUCTION

Colloidal dispersions consisting of micrometer-sized liquid crystal (LC) droplets dispersed in an aqueous phase (*i.e.*, LC-in-water emulsions) have been used extensively as analytical sensors to determine the presence of a range of aqueous analytes.[1–5] Adsorption of chemical and biological species at the LC-water interface may alter the surface anchoring, which results in reorganization of the internal ordering of the LC droplets from a so-called bipolar configuration to a radial configuration (with intermediate geometries being also possible). Because LCs possess anisotropic optical properties (birefringence), this configurational transformation of the LC droplets leads to a distinct change in their optical appearance that can be characterized by polarized light microscopy and used as feasible sensing technique.

The ordering transitions and consequently the optical transformations in the droplets of the nematic thermotropic LC 4-cyano-4'-pentylbiphenyl (5CB), for example, can be induced by amphiphilic species (*e.g.*, surfactants[6–8] and lipids[9,10]) or biological analytes (including proteins,[11–14] bile acids,[15]charged macromolecules,[16] viruses,[17] and bacterial endotoxins[1]). While recent studies have demonstrated the potential of LC droplets as a simple yet sophisticated analytical tool for the detection of a variety of different analytes, the current methods are not optimal for quantitative analysis of the configurational states of LC droplets. This is because bare, free-floating droplets of LC-in-water emulsions are metastable and undergo coalescence over a short period of storage time, leading to the formation of larger LC droplets (> 10 μm) that do not exhibit an analyte-triggered ordering transition.[2] An additional technical challenge is associated with the sedimentation of LC droplets onto the glass cover slides that can be observed during microscopy measurements. The droplet sedimentation impedes accurate quantitative analysis of the LC ordering transitions. For instance, previous studies have demonstrated that interactions of the LC

droplets with the glass perturbs the configurations of the droplets[2,18,19] and, therefore, it is necessary to avoid imaging the adsorbed LC droplets near the cover slips.

Extensive research efforts have been made to address these issues, ranging from studies on LC emulsions stabilized by amphiphilic polymer adsorption[20–26] and layer-by-layer deposition of polyelectrolyte[6,16] to LC infusion into the preformed and semipermeable polymer microcapsules.[7,27,28] Recently, gel film dispersed LC droplets have been developed as a simple and label-free optical probe to report the presence of chemical and biological analytes.[29,30] This strategy involves embedding LC droplets within a gel matrix that limits droplet mobility and thus, delays their coalescence. These approaches permit the formation of large populations of stable LC droplets, mediate tuneable LC responses to analytes and hinder the interactions between droplets and glass surfaces. However, these polymer-integrated colloidal LC systems also introduce several fundamental properties and new behaviour that are found to be substantially different from those of bare LC droplets. Therefore, continued effort is required for the development of new LC droplet-based systems for effective detection of chemical and biological species.

One promising approach to create stable LC emulsions is to decorate the droplets by deformable microgel particles *via* the so-called Pickering stabilization mechanism. The uniqueness of such emulsions is that when particles adsorb at the fluid-fluid interface, the detachment energies are in the order of several thousands of kinetic energy units (k_BT, where k_B is Boltzmann constant and T is temperature) making the particles practically impossible to desorb.[31] In other words, this irreversible adsorption of particles might allow Pickering LC emulsions to have outstanding stability against droplet coalescence for several months.

In our previous work, we have demonstrated the stabilization of LC emulsions by soft and responsive poly(N-isopropylacrylamide) (PNIPAM) microgels, followed by the penetration of

small molecules through the adsorbed layer into the LC droplets.[32] These microgels enabled reversible stabilization and breakage of emulsions on demand by changing temperature or pH, and thus offering an opportunity to recycle the particles. Although PNIPAM microgel-stabilized Pickering LC droplets exhibit extraordinary stability with precise control over size and interfacial chemistry, they are unsuitable to use in living organisms due to their limited biocompatibility. As a part of continued investigations into Pickering LC emulsion stabilization, we propose another class of protein-based, soft, biocompatible colloidal particles, i.e., whey protein microgel (WPM), to stabilize the LC emulsions for the first time.

Colloidal WPM particles can be prepared using a top-down method through controlled shearing of a physically cross-linked heat-set protein hydrogel by exploiting cysteine chemistry, *i.e.,* sulfhydryl-disulfide interchanges and hydrophobic interactions.[33–39] Typically, the sizes of these microgels are in the sub-micron range, down to tens of nanometers, and thus they are sometimes also referred to as nanogels.[36] Recently, WPM has emerged as one of the new generation of soft materials in food and biomedical applications because of their combined advantages of biocompatibility, tuneable physicochemical and material properties, size, porosity and permeability towards biomolecules such as digestive enzymes.[34–38,40,41] In addition, these soft colloidal particles have been shown to adsorb spontaneously to oil-water interfaces, forming a dense viscoelastic layer, and thus offering an exceptional stability against oil droplet coalescence.[40,42,43] These unique features provide us with an exciting opportunity to stabilize LC emulsions with WPMs making the system highly desirable for biomedical applications. To the best of our knowledge, investigations of LC emulsion stabilization by WPMs and the ability of such an assembly to respond to small molecules have not yet been explored in the literature.

In this work, we present a novel approach to the stabilization of micrometer-scale LC droplets by employing WPMs, which are known to act as efficient stabilizers for oil-in-water[35,40] or water-in-water[44] emulsions. These soft materials, due to their smaller size and biocompatibility, might provide unique features to the LC droplets in addition to the hypothesized exceptional stability. Our experiments sought to explore the potential of this approach towards droplet stability and characterize the impacts of WPM coating on the interfacial properties and internal ordering of the LC droplets, including their ability to respond to the presence of aqueous analytes. Stabilization of LC droplets with WPM particles allowed the small molecules (for instance sodium dodecyl sulfate (SDS)) to diffuse through the interfacial layer of WPM such that the LC droplets underwent an analyte-induced ordering transition. Despite promoting emulsion stability, the WPM coating hindered the droplet-surface interaction and therefore sedimentation/adsorption of the droplets onto the bottom surface could not influence the LC director configuration. Our results revealed that the response of WPM-coated LC droplets could be tuned by varying the number of droplets exposed to the aqueous analytes and the type of analytes, such as anionic SDS, cationic dodecyltrimethylammonium bromide (DTAB) and non-ionic tetra(ethylene glycol)monododecyl ether ($C_{12}E_4$). We further demonstrate the role of excess unadsorbed WPMs in limiting this response and an enhanced detection threshold upon removal of these free particles from the continuous phase. Overall, this unprecedented approach facilitated the analysis of configurational transitions of the LC droplets triggered by aqueous analytes, thus offering a highly feasible colloidal platform that could enable the development of new classes of biocompatible LC droplet-based optical sensors.

MATERIALS AND METHODS

Materials. Whey protein isolate (WPI) with 96.5% protein content was kindly gifted by Fonterra Cooperative, New Zealand. 4-cyano-4'-pentylbiphenyl (5CB), sodium dodecyl sulfate (SDS), dodecyltrimethylammonium bromide (DTAB), tetra(ethylene glycol)monododecyl ether ($C_{12}E_4$), sodium azide and Fast Green were purchased from Sigma-Aldrich Company, Dorset, UK. For microscopy measurements, Grace Bio-Labs secure seal imaging spacers and glass coverslips (12 mm) were obtained from VWR, UK. Milli-Q water (purified by treatment with a Milli-Q apparatus, Millipore, Bedford, UK) with a resistivity of 18.2MΩ cm at 25 °C was used for all experiments.

Preparation and characterization of whey protein microgel particle (WPM). WPMs were prepared with a slight modification of the top-down approach used in previous studies.[36,37] Briefly, whey protein isolate (WPI) powder was dissolved in Milli-Q water (15 wt % protein) with continuous stirring for 2 h. The WPI solution was heated at 90 ℃ for 30 min to form WPI gels via disulphide crosslinking and hydrophobic interactions, cooled to room temperature, and then stored at 4 ℃ overnight. The gels were mixed with Milli-Q water (1:4 w/w) and were broken down using a blender (HB711M, Kenwood, UK) for 5 minutes at 'Level 3' to create macroscopic gel particles. Further, the gel dispersion was homogenized using two passes through a Panda homogenizer (GEA Niro Soavi Homogeneizador Parma, Italy) with a two stage pressure of 250/50 bar. The resulting 3 wt % WPM aqueous dispersion was diluted to 0.005 – 1.0 wt % for emulsion preparation.

A Malvern Zetasizer Nano-ZS (Malvern Instruments Ltd, Worcestershire, UK) instrument operating at a detection angle of 173° with a light source of 633 nm He-Ne laser was used to determine the hydrodynamic diameter of WPM particles in aqueous medium by dynamic light scattering (DLS) at 25 °C. The stock WPM dispersion was diluted to 0.01 wt % particle

concentration with Milli-Q water for the measurement. The hydrodynamic diameter (D_h) of the droplets was calculated using the Stokes–Einstein equation:

$$D_h = \frac{k_B T}{3\pi\eta D_t} \quad (1)$$

where, D_t is the translational diffusion coefficient, k_B is the Boltzmann's constant, T is the temperature, and η is the viscosity of the medium. The refractive index of WPM and the dispersion were assumed to be 1.54 and 1.33, respectively.[37] The absorbance of the protein was set at 0.001.

To calculate the mesh size of the WPM, a frequency sweep test was performed from 0.1 to 100 Hz for the WPI heat-set gel from which the WPM was produced. The rheological mesaurements were performed using a Kinexus rheometer (Malvern Instruments Ltd, Worcestershire, UK) equipped with a 60 mm diameter cone and plate geometry at 0.5% strain at 25 °C. All the measurements were carried out at least five times on triplicate samples in order to calculate the mean and standard deviation.

Interfacial tension and interfacial shear viscosity of WPM. Interfacial tension (γ) measurements were performed using *n*-tetradecane in the presence of 0.5 wt% WPM using the pendant drop method in a Dataphysics OCA tensiometer (DataPhysics Instruments, Germany). A bended needle in the upward direction was used to immerse a drop of the lower density liquid (*n*-tetradecane) into the higher density Milli-Q water, latter containing 0.5 wt% WPM. The contour of the drop was extracted using the SCA 22 software and fitted to the Young-Laplace equation to obtain γ. The measurement was carried out in triplicate in order to calculate the mean and standard deviation.

The interfacial shear viscosity of WPM at *n*-tetradecane-water interface was measured using a two-dimensional Couette-type viscometer as reported previously.[36] The interfacial viscometer was operated in a constant shear-rate mode and a layer of pure *n*-tetradecane was layered over an aqueous solution of WPM (0.5 wt%) or non-microgelled WPI (0.5 wt%). A stainless steel biconical disk (radius 14.5 mm) was suspended from a thin torsion wire with its edge in the plane of the *n*-tetradecane-water interface of the solution contained within a cylindrical glass dish (radius 72.5 mm). The deflection of the disk was measured by reflection of a laser off a mirror on the spindle of the disc onto a scale at a fixed distance from the axis of the spindle. The constant shear rate apparent interfacial viscosity, η_i, is given by the following equation:

$$\eta_i = \frac{g_f}{\omega} K(\theta - \theta_0) \qquad (2)$$

where, K is the torsion constant of the wire, θ is the equilibrium deflection of the disc in the presence of the film, θ_0 is the equilibrium deflection in the absence of the interfacial film, *i.e.* due to the drag force of the sub-phase on the disc, g_f is the geometric factor, and ω is the angular velocity of the dish. A fixed value of $\omega = 1.27 \times 10 - 3$ rad s^{-1} was used and the measurements were carried out in triplicate in order to calculate the mean and standard deviation.

Preparation of the liquid crystal (LC) emulsions. The emulsions were prepared by mixing 10 µL of 5CB with aqueous dispersions of WPM (5 mL) of varying concentration (0.005 to 1 wt %) using an Ultra Turrax T25 homogenizer with a 10 mm head (S25N-10G) operated at 8,000 rpm for 2 min at room temperature. The LC emulsions with no additional WPM were used as controls. These bare water-dispersed LC emulsions were prepared by emulsification of 5CB in

200 water without the addition of any emulsifying agent. Although, these droplets were unprotected,
201 they remained stable against coalescence for at least 3 h and therefore, were used within this time.[3]
202 **Confocal laser scanning microscopy (CLSM).** The WPM-stabilized LC emulsions were
203 characterized using a Zeiss LSM880 confocal microscope (Carl Zeiss Micro Imaging GmbH,
204 Germany) operating at an inverted mode. The WPM was stained using an aqueous solution of Fast
205 Green (1 mg mL^{-1}) to a final concentration of 0.1 mg mL^{-1}. The samples (8 μL) were placed
206 between a cover glass and bottom coverslip (thickness 170 μm), and hermetically sealed by using
207 a 120 μm thick spacer with a 51 mm aperture (Secure Seal Imaging). A pinhole diameter of 1 Airy
208 Unit was maintained to filter out any background light originating from the excitation laser. The
209 samples were excited at 633 nm and the florescence images were collected using an oil immersion
210 63× objective at 25 °C. The emitted fluorescent light was detected at 660–710 nm.
211 **Cryogenic scanning electron microscopy (cryo-SEM) measurements.** A cryo-SEM
212 microscope (Quanta 200 F scanning electron microscope, FEI, Eindhoven) was used to directly
213 observe the arrangement of WPM in an aqueous dispersion and at the surface of the LC emulsion
214 droplets. A drop of aqueous dispersion of WPM (20 vol%) or LC-in-water emulsion stabilized by
215 0.005 or 1.0 wt % WPM was placed into a copper holder, and then plunge-frozen on a bed of dried
216 ice using liquid nitrogen (-180℃). The frozen sample was transferred to the sample preparation
217 unit operating at -160 °C and a pressure of 10^{-6} mbar. Finally, the sample was placed into the
218 observation chamber equipped with an SEM cold stage module at -135 °C for imaging. Once the
219 sample was fractured, the temperature of the observation chamber was raised to -110 °C for
220 approximately 15 min and the sample was placed for observation.
221 **Droplet size and polydispersity measurements of LC emulsions.** The LC emulsions
222 were observed with a Leica DM2700 optical microscope in transmission mode fitted with a Nikon

D7200 camera. The samples were prepared in the same way as described for the confocal laser scanning microscopy experiments. Bright field images of at least 100 droplets for each sample were recorded and analysed using the 'Image J' software. The surface average diameter ($D_{[3,2]}$) and the polydispersity (*PDI*), defined by eqs (3) and (4), respectively were calculated.

$$D_{[3,2]} = \frac{\sum_i N_i D_i^3}{\sum_i N_i D_i^2} \quad (3)$$

$$PDI = \frac{1}{D_m} \frac{\sum_i N_i D_i^3 |D_m - D_i|}{\sum_i N_i D_i^3} \quad (4)$$

where, N_i is the total number of droplets with diameter D_i. D_m is the median diameter, *i.e.* the diameter for which the cumulative undersized volume fraction is equal to 50%.

Determination of surface coverage by WPM particles. In order to obtain the surface coverage of LC droplets by WPM, the concentration of unadsorbed WPM particles left in the continuous phase of emulsions was determined. The WPM-stabilized Pickering LC-in-water emulsions were centrifuged at 6,000 rpm (3824 *g*) for 15 min at 25 ^{o}C (Eppendorf 5430, Germany). Using a syringe, the supernatants were carefully removed and filtered using 0.45 μm pore size filters (Millipore Corp., USA). The concentration of WPM in the supernatants was determined using a standard Bradford assay kit (HiMedia). The absorbance of the samples was recorded on a Genesis 180 UV-Vis Spectrophotometer (Thermo Fischer, Germany) at 595 nm. The amount of adsorbed WPM at the interface was obtained from the difference between the amount of WPM used to prepare the emulsions and that measured in the supernatants. The adsorption efficiency (α) was calculated as the ratio of the amount of WPM adsorbed at the interface to the total amount of

WPM used during the initial emulsion preparation. The surface coverage, $\Gamma_{595\ nm}$ (mg m^{-2}) was estimated using a simple mass balance equation.[45]

$$\Gamma_{595\ \mathrm{nm}} = \left(\frac{1-\phi}{6\phi}\right) D_{[3,2]} c_{adsorb} \quad (5)$$

where, ϕ is the volume fraction of the disperse phase, $D_{[3,2]}$ is the mean droplet diameter, and C_{adsorb} is the concentration of WPM adsorbed at the interface.

ζ-potential measurements. The zeta-potential values of WPM particles and WPM-coated LC droplets were determined at 25 °C using a Malvern Zetasizer Nano-ZS instrument equipped with a 4 mW He-Ne laser (633 nm). The samples were placed into a folded capillary cell (DTS 1070) and the measurements were carried out at an angle of 173°. Before the measurements, the WPM sample was diluted to 0.003 wt % particle concentration and the emulsions were diluted 5-folds. Assuming all the particles or droplets were spherical, the electrophoretic mobility in the solution was recorded. The zeta-potential was then calculated from the measured electrophoretic mobility using the Smoluchowski equation.[46] Three individual measurements on triplicate samples were taken in order to calculate the mean and standard deviation for each sample.

Determination of internal configuration of LC droplets. The internal ordering of the LC emulsions was characterized by polarized light microscopy as described previously.[32] Briefly, 500 µL aqueous dispersion of LC droplets was added to the surfactant solutions (or Milli-Q water for control) of different concentrations to prepare a sample containing ~2× 10^6 mL^{-1} droplets. The emulsions were washed to eliminate the interference of unadsorbed WPM. In order to investigate the effect of droplet concentration on the LC response to SDS, different amount of LC emulsion

droplets prepared at a fixed WPM concentration (0.01 wt %) were added to the SDS solutions. The samples were kept at room temperature for 30 min allowing the analytes to adsorb at the LC-water interface, and thereby inducing the LC response.[16] An aliquot (8 μL) was used to prepare the samples as described for the confocal scanning laser microscopy experiments. The configurations of the LCs within the emulsion droplets were determined by observation of the droplets using a Leica DM2700 optical microscope equipped with an objective magnification power of 100× (an oil-immersion lens) under cross polarizer. Polarized light micrographs of at least 100 droplets for each sample were recorded with a Nikon D7200 camera and analysed using the 'Image J' software. The size distributions as well as quantification of the configurational states of the LC droplets were determined by statistical analysis.

Statistical analysis. The statistical software SPSS software (IBM, SPSS statistics, version 24) was used. All experimental results were reported as means with standard deviations of at least three measurements on triplicate samples (n = 3 × 3). The significant difference between samples were considered when $p < 0.05$ as per Tukey's test.

RESULTS AND DISCUSSION

Characteristics of aqueous dispersion of WPM. As presented in Figure 1a, WPM showed a monodispersed particle size distribution with a peak ranging between 0.1 and 10 μm. The hydrodynamic diameter (D_h) of WPM was found to be ~ 90 nm with a low polydispersity index ($PDI < 0.12$). The D_h obtained by DLS was in close agreement with that obtained in cryo-SEM measurements (Figure 1b). The microgels produced by the top down approach were largely spherical (Figure 1b), however, showed some tendency to aggregate in the observation grid. Such aggregation might be associated with the effects of sample preparation for cryo-SEM on particle

morphology, which was not evident from the monomodal distribution obtained in DLS (Figure 1a). The aqueous dispersion of WPM exhibited a high colloidal stability with negative ζ-potential value (-37.5 mV). The physicochemical properties of WPM are in good agreement with previous studies.[36,37]

Since, we are interested in investigating whether the stabilization by WPM would enable configurational transitions of the Pickering LC droplets when subjected to small molecular analytes such as SDS, it was important to determine the mesh size and consequently the modulus of the WPM through which these analytes could pass. In order to derive indirect information about the modulus of the WPM, the mechanical properties of the WPI heat-set gel was measured considering that WPM is an average monomeric unit of the WPI heat-set gel.[37] Figure 1c shows that WPI formed a viscoelastic gel (~ 10 kPa modulus) *via* thermal-crosslinking characterized by the predominance of storage modulus (G′) over loss modulus (G″), absence of crossover points between G′and G″, and also a weak frequency dependence. Based on the modulus of the WPI gels, the average mesh size of the WPM was calculated using eq (6):[47]

$$\xi^3 = \frac{k_B T}{G'} \quad (6)$$

where, ξ is the mesh size of WPM.

As can be seen in the schematic in the inset of Figure 1c, the calculated ξ of WPM was 6.5 nm. Therefore, it can be hypothesized that small molecules, with sizes generally below a few nanometers, should not have any tortuous restriction to access the LC-water interface if passing through the meshes of the WPM network itself.

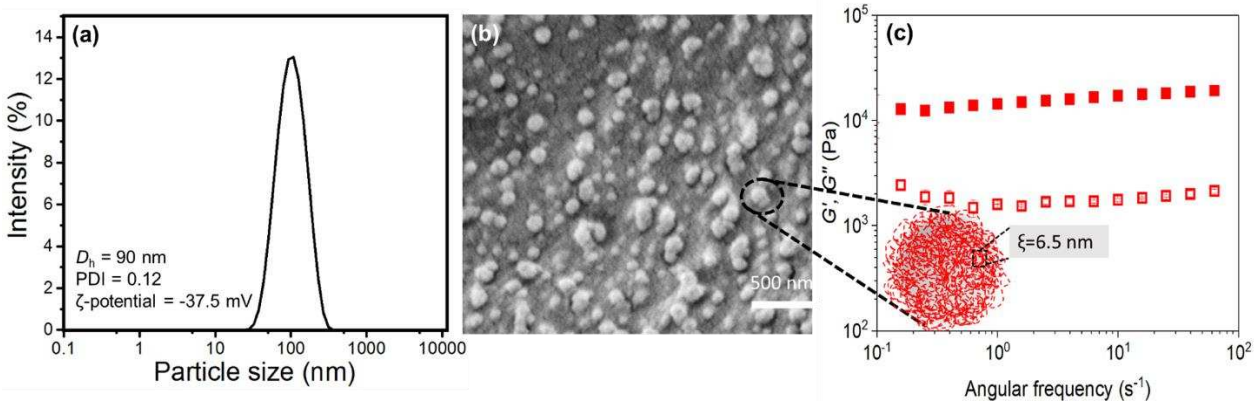

311

312 **Figure 1.** (a) Particle size distribution measured using DLS with insets representing the physicochemical properties
313 and (b) cryo-SEM image of WPM. (c) Frequency sweep of the heat-set WPI gel used to prepare WPM showing the
314 storage module, G′ (closed symbol) and loss modulus, G″ (open symbols) with inset schematic of the WPM showing
315 the mesh size (ξ) calculated using G′ of the heat-set WPI gel (c).

316 **Characteristics of Pickering LC-in-water emulsions stabilized by WPM.** WPM-
317 stabilized LC droplets were obtained by emulsifying a low molecular weight LC, nematic 4-cyano-
318 4'-pentylbiphenyl (5CB), with an aqueous dispersion of WPM. After emulsification, the location
319 of the WPMs in the LC emulsion droplets was determined by performing confocal laser scanning
320 microscopy (CLSM) using particles fluorescently stained with Fast Green. For this measurement,
321 the excess particles were washed out from the bulk phase to avoid signal emanating from the
322 unadsorbed microgels. As shown in Figure 2(a-d), the WPM-laden interface of the LC droplets
323 prepared with 0.005 wt % (Figure 2a and Figure 2b) and 1 wt % (Figure 2c and Figure 2d) appeared
324 fluorescent with green dots, whereas both the dispersed LC phase and the aqueous continuous
325 phase appeared as dark regions. These results suggest that the WPMs were adsorbed at the LC
326 droplet surface after emulsification and that the WPMs formed a uniform layer with complete
327 coverage at the interface irrespective of the WPM concentrations (0.005 – 1 wt %). Owing to the
328 very low volume ratio of LC to continuous phase, the number of WPM particles under the studied
329 concentrations were sufficient to coat the droplets effectively. Interestingly, the WPM coated-LC

droplets did not undergo any inter-droplet flocculation even at higher WPM concentration in contrast to the droplet aggregation reported for sub-micron particle-stabilized oil-in-water emulsions.[40]

The characterization of surface morphology of the WPM-coated LC droplets by cryo-SEM measurements allowed direct visualization of the Pickering particles at the surfaces of the LC droplets. The morphographs of the interface at 0.005 and 1 wt % WPM concentrations with various magnifications are presented in Figure 2(e-h). The presence of WPMs was clearly evident at the LC droplet surface, confirming Pickering stabilization. The particles formed a 2D network with sparsely distributed WPM aggregates at the interface (Figures 2e and 2g). The higher magnification images (Figures 2f and 2h), exhibiting cross-sections of the droplets, demonstrated that WPM adsorption at the LC droplet surface resulted in the formation of a thin and continuous layer of inter-penetrated particles. The topography appeared to vary significantly with WPM concentration: the interfacial layer adopted a discrete organisation of clearly distinguishable individual particles at low WPM concentration (0.005 wt %, Figure 2e), whereas, at higher WPM concentration (1 wt %, Figure 2g), a denser layer was evident, with limited appearance of individual particles at the interface.

In addition to the cryo-SEM and confocal imaging, we conducted interfacial shear rheology experiments to investigate formation and structuring of the particulate layers of WPM at the interface versus a conventional non-microgelled protein layer (Supporting Information Figure S1). The value of η_i for non-microgelled WPI decreased markedly from ~ 450 mN s m^{-1} within the first two hours to its quarter after 24 h, which was in line with previous report.[36] As might be anticipated from the microscopic results across length scales (Figure 2), the value of η_i for WPM at the *n*-tretadecane-water interface was twice as that of the non-microgelled system within the

first two hours ($p < 0.05$) and became almost an order of magnitude (1149 mN s m^{-1}) higher than that of the non-microgelled counterpart (147 mN s m^{-1}) in 24 h time scale ($p < 0.05$; Supporting Information Figure S1). These high values obtained for WPM was indicative of strengthening of the interfacial films by the presence of a network of adsorbed microgel particles. The quantitative results obtained using interfacial shear viscosity perfectly corroborated with the qualitative observation of WPM at the interface of the WPM-stabilized LC emulsions in the CLSM and cryo-SEM images. These results, when combined, led us to conclude that the WPMs were adsorbing at the LC droplet surface in a network arrangement, and that droplet stability was controlled most likely by the degree of WPM coating.

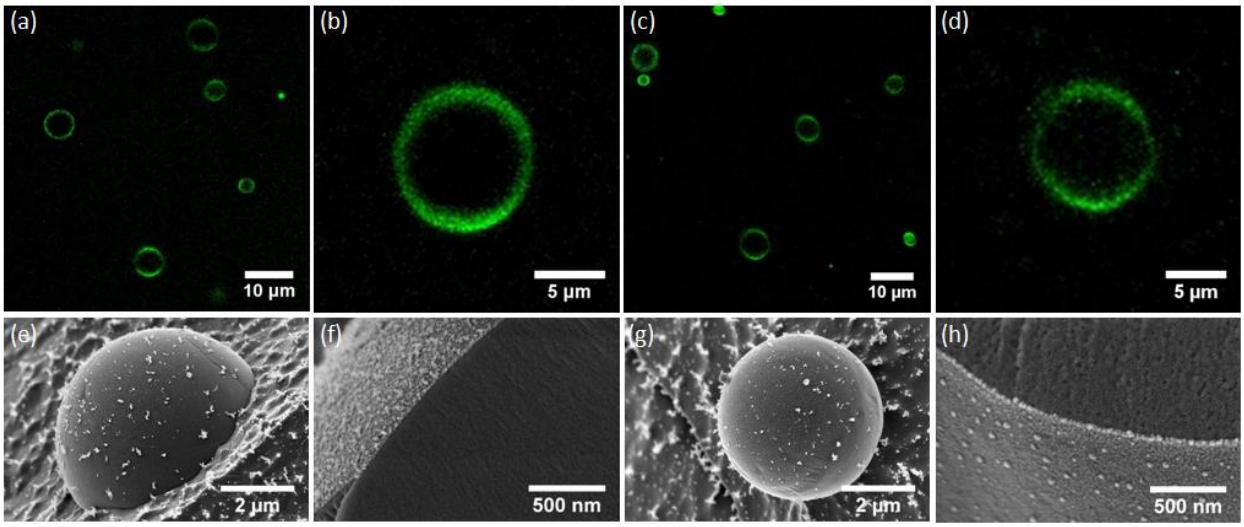

Figure 2. Confocal (a-d) and cryo-SEM (e-h) images of Pickering LC-in-water emulsion droplets stabilized by 0.005 (a,b,e,f) and 1 wt % (c,d,g,h) WPM obtained immediately after preparation. Confocal micrographs (a,c) show arrays of droplets dispersed in aqueous medium and (b,d) show the cross-section of single drop covered with WPM. Cryo-SEM morphographs (e,g) show the external drop surface morphologies and (f,h) show the cross-section of the droplets covered by WPM.

The stability of the LC emulsions was investigated by determining the diameters ($D_{[3,2]}$) and polydispersity indexes (*PDI*) of the droplets over time. For this purpose, a series of emulsions were prepared with equal volume fraction of LC phase and different concentrations of WPM (0.005 – 1 wt %). Figure 3 shows the optical microscopy images of freshly prepared LC droplets at different initial WPM concentrations in the aqueous phase. The corresponding $D_{[3,2]}$ and *PDI* values calculated from eq (3) and (4), respectively are presented in Table 1. The $D_{[3,2]}$ and *PDI* values for bare LC droplets increased from 13.5 to 32.3 µm ($p < 0.05$) and 3.5 to 8.7 % ($p < 0.05$), respectively over a period of 14 days (Supporting Information Figure S2 and Figure S3). Bare LC emulsions underwent coalescence over time, leading to the formation of larger droplets with a broader size-distribution (Supporting Information Figure S2 and Figure S3). On the other hand, the LC droplets that were covered by WPM did not change their size significantly ($D_{[3,2]} \leq 11.2$ µm, $p > 0.05$), and maintained a narrow size-distribution after two weeks ($PDI \leq 3.6$ %, $p > 0.05$). The WPM remained adsorbed at the interface over a period of two weeks as characterized by confocal microscopy (Supporting Information Figure S4). The WPM adsorbed spontaneously to the interface, where they reduced the interfacial tension to ~ 13.5 mN m^{-1} for *n*-tetradecane-water interface (Supporting Information Figure S5) in line with previous reports[36,40] and formed a dense viscoelastic layer as previously discussed in the interfacial shear rheology results (Supporting Information Figure S1). The irreversible adsorption of WPM at the interface offered resistance against coalescence of the LC droplets, thus providing a remarkable stability.

Interestingly, the initial size ($D_{[3,2]}$ values) of the LC droplets stabilized by WPM decreased slightly from 10.8 to 6.5 µm ($p > 0.05$) as the concentration of the particles increased from 0.005 to 1 wt %. A similar trend was also observed with the two-week old WPM coated LC droplets. The presence of higher initial WPM concentration led to the formation of a dense WPM layer

392 (Figure 2h) at the interface with high surface coverage (Table 1), thereby decreasing the average
393 droplet size but raising the total interfacial area. Thus, the WPMs were allowed to cover a much
394 larger area, resulting in a lower droplet-size with enhanced stability and increased number of
395 Pickering LC-droplets.
396

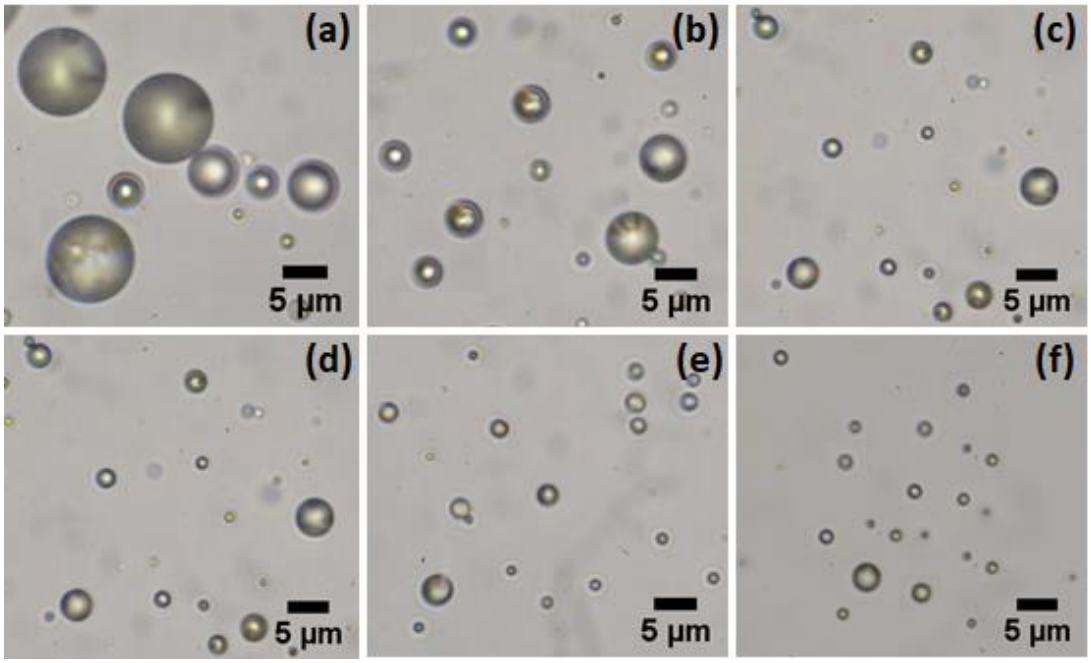

397

398 **Figure 3.** Optical microscopy images (bright field) of freshly prepared Pickering LC-in-water emulsion droplets
399 stabilized by (a) 0, (b) 0.005, (c) 0.01, (d) 0.05, (e) 0.1 and (f) 1 wt % WPM.

400 **Table 1. Characteristic parameters of Pickering LC-in-water emulsions stabilized by different concentration**
401 **of WPM***

[WPM] (wt %)	$D_{[3,2]}$ (µm)	*PDI* (%)	ζ-potential (mV)	α (%)	$\Gamma_{595\ nm}$ (mg m^{-2})
0.005	10.8 ± 1.1 [a] (11.2 ± 1.6) [a]	3.2 ± 0.7 [b] (3.6 ± 0.4) [b]	-36.3 ± 2.1 [c] (-37.3 ± 2.7) [c]	61.1 ± 0.3 [d]	27.6 ± 0.1 [g]
0.01	9.9 ± 1.5 [a] (9.6 ± 0.8) [a]	4.4 ± 0.9 [b] (2.3 ± 0.8) [b]	-32.7 ± 4.1 [c] (-32.4 ± 3.4) [c]	62.1 ± 0.1 [d]	50.9 ± 0.1 [h]

0.05	8.7 ± 1.6 [a] (8.8 ± 0.2) [a]	3.1 ± 0.7 [b] (2.4 ± 0.6) [b]	-28.5 ± 3.1 [c] (-26.1 ± 1.7) [c]	81.6 ± 0.3 [e]	294.6 ± 1.1 [i]
0.1	7.9 ± 1.4 [a] (7.6 ± 0.3) [a]	2.9 ± 0.8 [b] (2.0 ± 0.3) [b]	-27.1 ±2.9 [c] (-25.9 ± 2.1) [c]	91.3 ± 0.4 [e,f]	594.2 ± 2.5 [j]
1	6.5 ± 1.3 [a] (7.9 ± 0.2) [a]	3.5 ± 0.6 [b] (2.4 ± 0.5) [b]	-25.9 ± 2.8 [c] (-25.3 ± 2.0) [c]	98.8 ± 0.1 [f]	5368.7 ± 0.5 [k]

[*]The data without parentheses represent freshly prepared LC emulsions and that within parentheses represent LC emulsions after 14 days of storage post preparation. The values represent means ± standard deviations of at least three independent experiments on triplicate samples (n = 3 × 3). Samples with the same letter do not differ significantly ($p > 0.05$) according to Tukey's test.

As presented in Table 1, the particle adsorption efficiencies, α, at the LC droplet surfaces within the studied concentration range (0.005 – 1 wt %) were calculated to be < 100 %, indicating that significant amounts of unadsorbed WPM were present in the continuous phase. Furthermore, a progressive increase of the adsorption efficiency was observed with the increase of initial WPM concentration ($p < 0.05$; Table 1). This suggested that increased interfacial area of the LC droplets (lower $D_{[3,2]}$) at higher initial WPM concentration allowed a large number of WPM to adsorb at the interface. The surface coverage, Γ_{595nm}, calculated from eq (5) for the different formulations revealed that the particle density at the interface largely increased with increasing WPM concentration ($p < 0.05$; Table 1). We also determined the surface coverage value of ideal WPM monolayer at the interface, $\Gamma_{90\%}$, for comparison. This estimation was made on basis of the assumption that monodispersed and spherical WPMs were adsorbed in a hexagonal close packing arrangement with only 90 % of the interfacial area being covered. $\Gamma_{90\%}$ was calculated to be 8.1 mg m^{-2} using a WPM diameter of 90 nm obtained from the DLS data and protein density equal to 0.150 g cm^{-3}.[48] The particle densities at the LC-water interface, within the studied WPM

concentration range, were found to be significantly higher than that obtained for ideal monolayer coverage, *i.e.*, $\Gamma_{595\ nm} >> \Gamma_{90\%}$. This simple calculation of interfacial adsorption densities demonstrated (Table 1) that even at 0.05 wt % WPM, a 3× monolayer was formed at the LC-water interface which rose to nearly 50× monolayer at 1 wt %. As anticipated from the cryo-SEM images (Figure 2f and Figure 2h) and interfacial shear rheology measurements (Supporting Information Figure S1), the microgels were adsorbed either as small aggregates during the emulsification process or they re-formed a network of aggregates after reaching to the interface to achieve such high surface coverages, resulting in multi-layered interfaces.

Both the WPM and LC droplet surface were negatively charged with ζ-potential values of -37.5 and -35.6 mV ($p > 0.05$), respectively. Therefore, the particles had to cross an electrostatic barrier to adsorb at the interface. In this context, the hydrodynamic force that was generated by mechanical agitation, played an important role. This force acted against the repulsive electrostatic interaction and pushed the WPM towards the interface during the emulsification process.[49] Thus, the adsorption of WPM was associated with the balance between the electrostatic repulsive force and hydrodynamic force. As these forces were not only controlled by the charge but also by the particle size, the latter might become crucial in determining particle adsorption at the LC droplet surface. This hypothesis was supported by a past study on the specific case in which the two forces were of the same order of magnitude.[49] In addition, the molecular hydrophobic interaction between the LC and particles in the aqueous continuous phase facilitated particle attachment to the interface, thus leading to the formation of a WPM-laden LC-water interface.[50,51]

The absolute values of ζ-potential of all the WPM-stabilized Pickering LC droplets were found to be less than that of the aqueous dispersion of WPM (Table 1). Moreover, a gradual decrease of negative surface charge was recorded as the initial WPM concentration increased from

444 0.005 to 1 wt %. These findings further support our hypothesis that the interface was covered by a
445 network of particle aggregates, which would reduce the exposure of WPM charged units to the
446 aqueous environment, as captured during the electrophoretic measurements. Higher initial WPM
447 concentration led to the formation of a dense layer with increased degree of aggregation at the
448 interface, resulting in a decreased ζ-potential value. In line with other results of Pickering emulsion
449 stabilization, the WPM-coated LC droplets did not show any significant change in the ζ-potential
450 value after two weeks of storage ($p > 0.05$; Table 1). It is well known that sub-micron-sized
451 particles tend to reach the interface much more slowly as compared to classical surfactants but
452 once adsorbed they remain almost irreversibly attached. In order to visualize this in our systems,
453 confocal microscopy was conducted with samples containing aged (two weeks) WPM-coated LC
454 droplets. As shown in Supporting Information Figure S4, the WPM particles appeared as
455 aggregates; however, these clusters were closely associated with the droplet surfaces. Thus, the
456 LC droplets were sufficiently protected by a continuous multi-layered network of WPM aggregates
457 along with individual discernible microgel particles. These results suggested that ageing of the
458 WPM-coated LC droplets affected the particle integrity at the interface to a certain extent without
459 influencing the droplet stability.

460 It is clear that, within the explored WPM concentration range (0.005 – 1 wt %, particle-
461 rich regime), the LC droplets were sufficiently protected by a complete coverage of WPM particles
462 and were thus able to remain stable over time. Therefore, this entire concentration range was
463 selected to study whether or not the stabilization of LC droplets by WPM enabled molecular
464 diffusion through the interfacial layer to induce a configuration transition within the Pickering LC
465 droplets.

Analyte-induced ordering transition in the WPM-stabilized Pickering LC droplets. In order to determine the internal ordering of the LCs within the droplets that were decorated with WPM, the optical appearance of the droplets was evaluated using cross-polarized light microscopy. In absence of any analyte, the WPM-stabilized Pickering LC droplets exhibited a bipolar configuration as depicted in Figure 4a. In a bipolar droplet, the LCs are oriented parallel to the surface of the droplet, thus forming two diametrically opposite point defects (called boojums) at the poles of the droplet. Similar to the observation reported in our previous study on LC emulsions stabilized by poly(N-isopropyl acrylamide) microgels,[32] WPM adsorption did not influence the internal ordering of the LCs in the droplet, leading to a distinct bipolar optical signature.

After being exposed to 5 mM SDS solution (the anionic model analyte), the negative ζ-potential value of WPM-coated LC droplets increased significantly ($p < 0.05$; Supporting Information Table S1), suggesting the adsorption of SDS molecules at the interface. Interestingly, the addition of SDS could not remove the pre-adsorbed WPM particles from the interface as observed in confocal image (Supporting Information Figure S6), which might be attributed to the high detachment energies needed to remove the WPMs once adsorbed. In presence of 5 mM SDS, the WPM-coated LC droplets underwent a rapid ordering transition from the bipolar configuration to the so-called "radial" configuration as shown in Figure 4b. This radial configuration resulted in a homeotropic surface anchoring of the LCs (perpendicular director alignment to the surface of the droplet) with a single point defect at the center of the droplet, and yielded a characteristic optical signature (cross-like pattern) when viewed under crossed polarizer. The high surface activity allowed the anionic SDS to pass through the negatively-charged WPM layer to adsorb at the LC-water interface. Once at the interface, the SDS molecules extended their hydrophobic tails into the

LC phase, triggering an ordering transition in the WPM-coated LC droplets.[6,52] Thus, these results highlighted the potential of WPM-stabilized Pickering LC droplets to act as an optical sensor, for the first time in the literature.

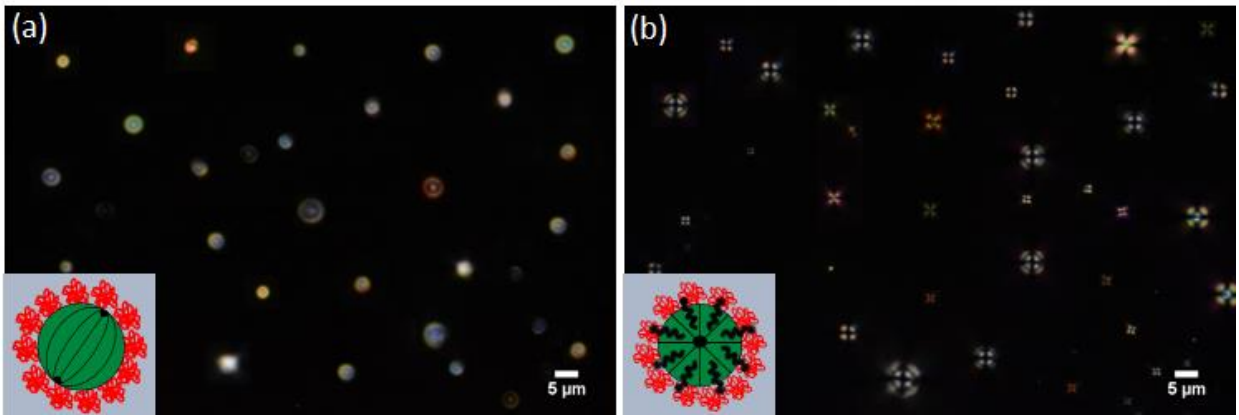

Figure 4. Polarized light microscopy images of the WPM-stabilized Pickering LC droplets (0.01 wt % WPM) dispersed in (a) SDS-free aqueous medium with bipolar signature and (b) 5 mM SDS solution with radial signature. The insets represent the schematic illustration of the WPM-stabilized Pickering LC droplets with respective internal droplet configurations.

As discussed in introduction, the droplet-surface interaction resulting from sedimentation/adsorption of bare water-dispersed LC droplets onto the bottom wall can strongly influence the LC configuration.[2,18] Although optical imaging of the adsorbed LC droplets is easy, such droplets cannot be taken into consideration for analysis of their configurational states as quantification of the aqueous analyte provides inaccurate results. Inspection of the adsorbed WPM-stabilized LC droplets (Supporting Information Figure S7) revealed that the LCs retained their original configuration within the droplets (*e.g.*, bipolar in absence of SDS and radial in presence of SDS) after depositing onto the glass cover slip. Thus, the WPM-laden interface avoided the droplet-glass surface interaction during interpretation of the configurational states of the LC droplets, enabling accurate quantification of the aqueous analyte.

The dynamic range of the WPM-coated LC droplet response to SDS was obtained by measuring the number of droplets that underwent bipolar-to-radial transition as a function of SDS concentration. In our experiments, LC emulsions prepared with various WPM concentrations, ranging between 0.005 – 1 wt % , were exposed to SDS solutions at a fixed droplet concentration (~2× 10^6 mL^{-1}). As shown in Figure 5a, the bipolar-to-radial transition of WPM-stabilized Pickering LC droplets, which was dependent on the SDS concentration, provided S-shaped dose-response curves. An additional significant finding obtained from these experiments was that the dynamic LC response to SDS shifted toward higher SDS concentration with increasing amount of WPM used during the emulsification process. The limit of detection, *i.e.*, the SDS concentration at which 50% of bipolar-to-radial transition in the LC droplets occurred, increased with the increase of WPM concentration (0.84, 1.86, 2.75, 3.5, 5 mM for 0.005, 0.01, 0.05, 0.1 and 1 wt % WPM-stabilized Pickering LC droplets, respectively, $p < 0.05$). Although bare LC droplets exhibited a lower detection limit for SDS (~0.15 mM), quantification of aqueous analytes using these unprotected droplets is not optimal due to their limited stability.

It is well established that SDS binds with the proteins by predominantly hydrophobic interaction in the sub-micellar concentration and this interaction is independent of the structure, conformation, and ionization state of the proteins.[53] The SDS molecules were assumed to bind with WPM by hydrophobic force, nevertheless both of them were negatively charged. Therefore, we hypothesized that SDS binding to the adsorbed as well as free WPM particles in the continuous phase may interfere with the response of WPM-stabilized Pickering LC droplets to SDS. This interaction potentially reduced the accessibility of SDS to the LC droplets and thus, reduced the configurational transition. For instance, one may argue that the presence of large amount of WPM may lead to the increased quantities of SDS binding to WPM, thereby reducing the LC response

to the remaining SDS. On the other hand, SDS is known to have strong affinity towards the LC-water interface due to the interaction of hydrophobic chain segment that penetrates deep into the LC phase.[4,52] Therefore, the adsorption of SDS at the WPM-laden interface was related to the subtle balance between the SDS-WPM and SDS-LC interactions. Here, SDS-LC interaction dominated over SDS-WPM interaction, thus allowing the SDS molecules to pass through the WPM layer and gain access to the LC-water interface.

To provide further insights into the role of adsorbed WPM on the configurational transition of LC droplets triggered by SDS, we performed an experiment in which the excess unadsorbed particles were removed from the aqueous continuous phase prior to exposing the WPM-coated droplets to SDS. This experiment sought to eliminate any possible interference of free WPM in the continuous phase. The droplet concentration was kept constant to avoid the effect of droplet number on the LC response to SDS. After washing off the excess unadsorbed WPM from the aqueous medium, the dose-response curves followed an identical trend (Figure 5b) as was observed in the presence of free particles. Interestingly, the WPM-stabilized Pickering LC droplets maintained a same detection limit (~0.85 mM, $p > 0.05$) irrespective of the initial particle concentration (between 0.005 – 0.1 wt % WPM). However, when the LC emulsions were prepared with 1 wt % WPM, the response was shifted to the right with a detection limit of 1.85 mM ($p < 0.05$). Although the average size of the droplets decreased with the increase of WPM concentration (Table 1), this variation was fairly small within the studied concentration range of WPM. Therefore, the effect of drop size on the LC response to SDS was assumed to be insignificant. It was only the particle density at the interface and consequently the interfacial interaction between SDS and WPM, which controlled the SDS penetration into the LC droplets and thus the configurational transition after removal of excess WPM from the bulk.

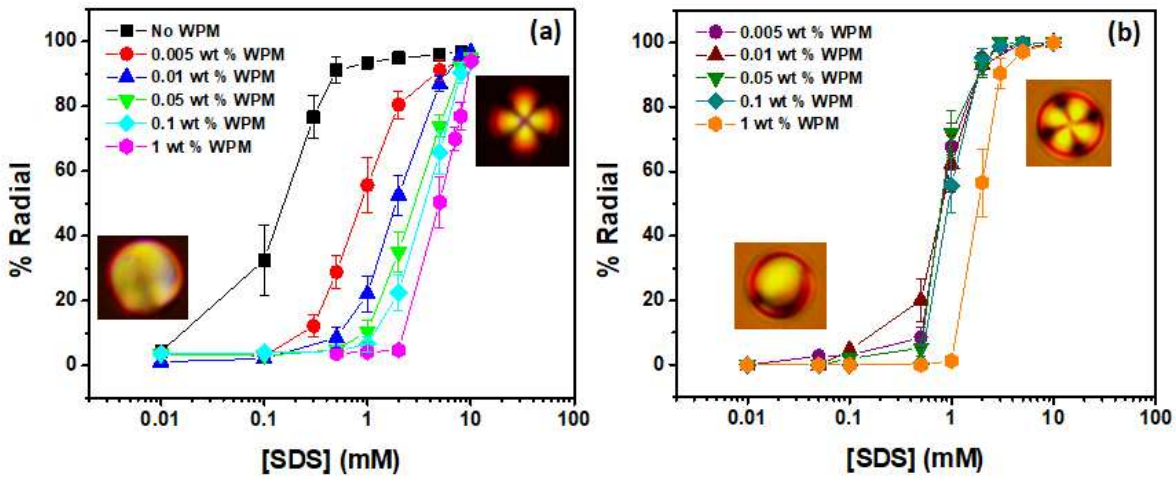

Figure 5. Dose-responses of WPM-stabilized Pickering LC droplets to SDS at different initial WPM concentrations (a) in presence of excess unadsorbed particles and (b) after removal of excess unadsorbed WPM particles from the continuous phase. The measurements were taken at a fixed droplet concentration of 2×10^6 mL^{-1}. The data points represent means ± standard deviations of at least three independent experiments on triplicate samples (n = 3 × 3).

Overall, inspection of the results presented in Figure 5 demonstrate that the unadsorbed WPM strongly influenced the detection limit of LC towards analyte and removal of free WPM from the bulk solution remarkably changed the LC response to SDS. For clarity, we have plotted the dose-response curves of 0.01 wt % WPM-stabilized Pickering LC droplets before and after washing off the unadsorbed particles together with that obtained with the bare LC droplets (Supporting Information Figure S8). The dynamic response shifted to the left with a lower detection limit after removing the unadsorbed WPM. The excess presence of WPM in the aqueous medium reduced the amount of SDS capable of inducing the bipolar-to-radial ordering transition due to bulk interaction between SDS and WPM, thus reducing the overall LC response. Notably, the removal of unadsorbed WPM markedly improved the response of Pickering LC droplets but not to the extent that was observed for bare LC droplets.

One has to consider two possible pathways here for the analytes to reach the LC when dealing with the surface-laden LC droplets, such as meshes in the WPM as well as pores at the

572 interface (*i.e.,* gap between the WPM particles). As demonstrated earlier, the particle densities at
573 the interface were significantly higher with surface coverages more than a monolayer within the
574 explored concentration range of WPM (Table 1), suggesting a limited interfacial pore availability
575 for SDS to diffuse through. However, the diffusion of SDS through the residual pores couldn't be
576 ignored. In addition, the mesh size of the WPM gel network (6.5 nm; inset, Figure 1c) was
577 relatively large and consequently, it might have also allowed the small molecules such as SDS to
578 pass through the porous WPMs to gain access to the LC-water interface. We note that SDS could
579 also bind with the adsorbed WPM at the interface and thus blocking the permeation of SDS into
580 the LC droplets. However, the SDS molecules at a certain higher concentration were still able to
581 diffuse through the pores of the WPM mesh, adsorb at the LC-water interface and induce a radial
582 configuration in the LC droplets. Compared to bare LC droplets, a large amount of SDS was
583 required for WPM-stabilized Pickering LC droplets to respond to SDS, resulting in a higher limit
584 of detection. A larger WPM concentration such as 1 wt % led to the formation of a highly loaded
585 WPM layer with increased interfacial interaction between SDS and WPM that largely blocked the
586 diffusion of SDS to the LC droplets to induce a configuration transition. Thus, the dose-response
587 curve of the WPM-stabilized Pickering LC droplets shifted towards higher SDS concentration
588 (Figure 5b).

589 Different concentrations of LC droplets prepared with a fixed WPM concentration (0.01
590 wt %) were exposed to SDS solutions to investigate the effect of droplet concentration on the LC
591 response to SDS. Figure 6a shows that the dose-response curves of WPM-stabilized Pickering LC
592 droplets that gradually shifted towards a lower SDS concentration with decreasing the number of
593 droplets, indicating a strong influence of total drop surface area on the configurational transition.
594 The detection limit of LC towards SDS was found to decrease sharply from 0.85 to 0.23 mM ($p <$

595 0.05) as the droplet concentration reduced from 2×10^6 to 4×10^5 mL^{-1} (Figure 6b). A further
596 decrease of droplet number to 8×10^4 mL^{-1} only led to a small change in the detection limit ($p >$
597 0.05). Thus, these results suggested the possibility of tuning the response towards designing a
598 surface-laden biocompatible LC based assay using WPM for the sensitive detection of biological
599 analytes.

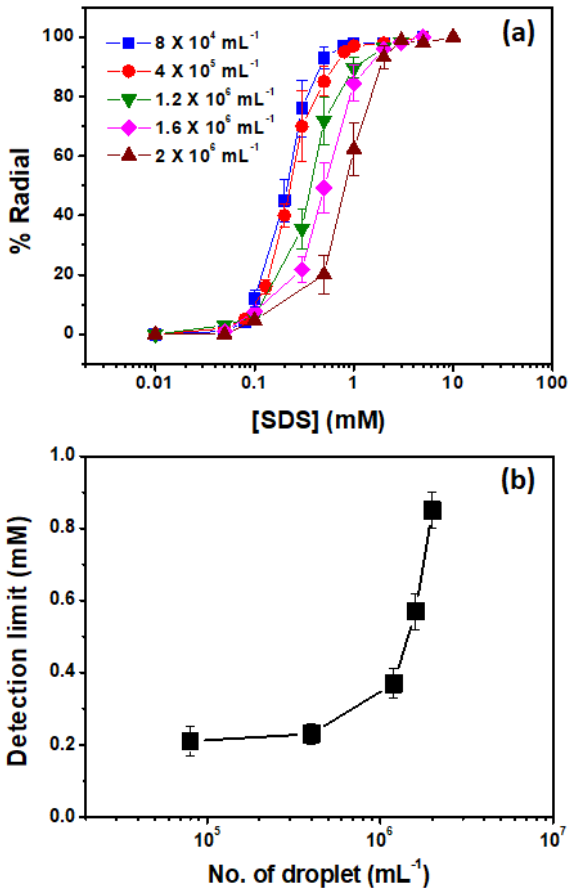

600

601 **Figure 6.** (a) Dose-response of WPM-stabilized Pickering LC droplets (0.01 wt % WPM) to SDS measured at different
602 droplet concentrations and (b) detection limit of WPM-coated Pickering LC droplets as a function of droplet number
603 exposed to SDS. The data points represent means ± standard deviations of at least three independent experiments on
604 triplicate samples (n = 3 × 3).

605

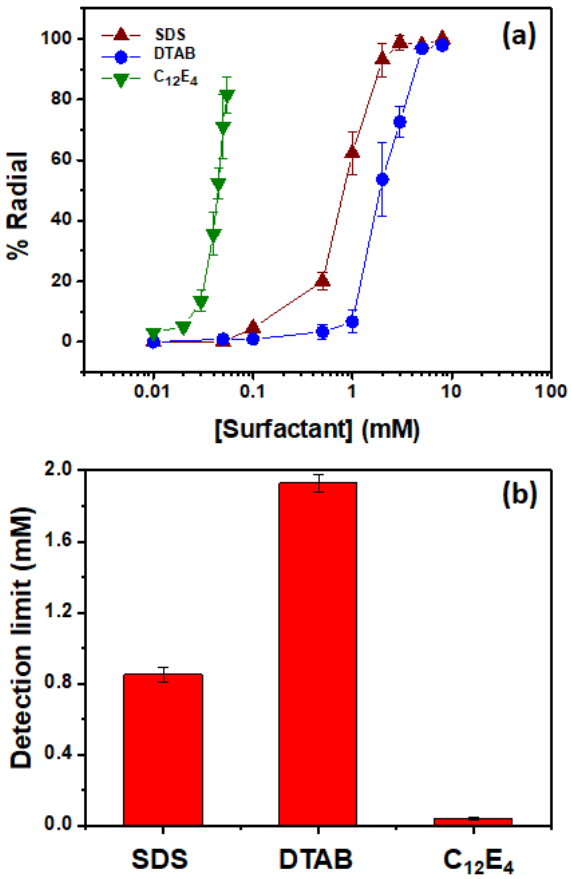

606

607 **Figure 7.** (a) Dose-response curves of WPM-stabilized Pickering LC droplets (0.01 wt % WPM) for SDS, DTAB and
608 $C_{12}E_4$ measured at a fixed droplet concentration of 2×10^6 mL^{-1} and (b) detection limit of WPM-coated Pickering LC
609 droplets for SDS, DTAB and $C_{12}E_4$. The data points represent means ± standard deviations of at least three independent
610 experiments on triplicate samples (n = 3 × 3).

611

612 While the LC response to anionic SDS was controlled by hydrophobic interaction between
613 SDS and negatively charged WPM at the interface, it was important to understand whether or not
614 the analytical ability of WPM-stabilized LC droplets was broadly useful for other surfactants in
615 addition to SDS. We found that other type of surfactants such as cationic DTAB and non-ionic
616 $C_{12}E_4$ were also able to induce configurational transitions in the WPM-stabilized Pickering LC
617 droplets. The adsorption of DTAB on the WPM-laden LC-water interface was confirmed by the

618 change of the ζ-potentials of the droplets from negative to positive values after exposing them to
619 DTAB ($p < 0.05$; Supporting Information Table S1). As expected, the ζ-potential of the surface-
620 laden LC droplets remained unaltered after the addition of $C_{12}E_4$. It is worth noting that each of
621 these surfactants tested have same tail length but differ in the head groups. Therefore, we compared
622 the configurational transitions of the Pickering LC droplets caused by SDS, DTAB, and $C_{12}E_4$ to
623 gain insights into the effect of head group types on the LC response. Figure 7a shows the dose-
624 response curves of 0.01 wt % WPM-stabilized LC droplets for three different types of surfactants,
625 in which the droplet concentration was kept constant (~2×10^6 mL^{-1}). The limit of detection limits
626 for SDS, DTAB, and $C_{12}E_4$ were found to be 0.85, 1.93 and 0.04 mM, respectively (Figure 7b).
627 Note, the dose-response experiment of LC to $C_{12}E_4$ was not possible to proceed above the critical
628 micellar concentration of $C_{12}E_4$ (0.05 mM) because of LC solubilisation in the micellar phase.
629 The variation of detection limit might reflect the differences in the affinity of the surfactants
630 to the WPM-laden LC-water interface. This trend of detection limit could be correlated with that
631 obtained when the experiments were performed with bare LC droplets (0.15 mM for SDS, 0.52
632 mM for DTAB, and 6 μM for $C_{12}E_4$; Supporting Information Figure S9). This suggested that the
633 observed difference was primarily attributed to the different surface properties of the surfactants.
634 Another aspect to consider when dealing with WPM-laden LC droplets was the interfacial
635 interaction that the surfactants had to overcome to adsorb at the LC-water interface. Cationic
636 DTAB was expected to bind strongly with the negatively-charged WPM at the interface by both
637 electrostatic and hydrophobic interactions. These interactions between DTAB and WPM largely
638 blocked the permeation of DTAB molecules into the LC droplets as compared to SDS. Whereas,
639 in the case of $C_{12}E_4$, the electrostatic force was insignificant and only the hydrophobic interaction
640 controlled the access of $C_{12}E_4$ to the LC droplets. Furthermore, $C_{12}E_4$ is known to adsorb strongly

at the oil-water interface at the lowest concentrations, contrary to SDS and DTAB.[54] Therefore, $C_{12}E_4$ was expected to diffuse more easily through the WPM layer to gain access to the LC-water interface.

CONCLUSIONS

We have demonstrated that a new class of soft biocompatible microgels can be employed to stabilize micrometer-sized LC droplets via Pickering mechanism for optimum quantification of aqueous analytes. The stabilization of LC droplets by WPM uniquely allowed the transport of small analytes such as SDS to the LC-water interface and thus, the LC droplets underwent an analyte-induced bipolar-to-radial ordering transition. Our results demonstrated that the meshes within the WPM as well as interfacial holes were being utilized as pathways through which the surfactant molecules could diffuse to access the LC droplets. The interaction between SDS and WPM in the bulk as well as at the interface that altered the access of SDS to the LC-water interface strongly influenced the configurational transition of the Pickering LC droplets. Further, the dose-response was found to be dependent on the number of droplets exposed to the aqueous analytes as well as the type of surfactant, such as anionic SDS, cationic DTAB and non-ionic $C_{12}E_4$. Overall, our findings address key issues associated with the stability, adsorption, characterization and analysis of configurational transitions in LC droplets, and pave the way for design of a surface-laden biocompatible LC droplet-based sensing platform for sensitive detection of aqueous analytes. Ongoing studies are investigating the role of LC droplet size on their ability to analyze small molecular surfactants and also the time scale of re-configuration of Pickering LC droplets as compared to the naked LC droplets.

SUPPORTING INFORMATION

Zeta-potentials of WPM-stabilized LC-in-emulsions in presence of SDS and DTAB, respectively; interfacial shear viscosities at *n*-tetradecane-water interface in presence of non-microgelled WPI and WPM; size distribution of freshly prepared LC-in-water emulsion droplets stabilized by various concentrations of WPM and after 14 days of storage, respectively; confocal microscopy images of LC-in-water emulsion droplets stabilized by various concentrations of WPM at different magnifications measured after 14 days of storage post preparation; interfacial tension between MilliQ water and *n*-tetradecane in presence of WPM; confocal microscopy images of LC-in-water emulsion droplets stabilized by 0.01 wt % WPM in absence and presence of SDS, respectively; polarized light microscopy images of WPM-stabilized LC droplets deposited on the bottom surface from aqueous dispersion in absence and presence of SDS, respectively; dose-response curves of 0.01 wt % WPM-stabilized LC droplets for SDS before and after removal of excess unadsorbed WPM from the aqueous medium, and further that obtained with bare LC droplets (no WPM coating) at a fixed droplet concentration of 2×10^6 mL^{-1}; dose-response curves and detection limits of bare LC droplets for SDS, DTAB and $C_{12}E_4$.

AUTHOR INFORMATION

Corresponding Authors

Email: abhijit@pu.ac.in (A.D.)†; A.Sarkar@leeds.ac.uk (A.S.) ‡

†Department of Chemistry and Centre for Advanced Studies in Chemistry, Panjab University − Chandigarh, Sector 14, Chandigarh, 160014, India

‡Food Colloids and Bioprocessing Group, School of Food Science and Nutrition, University of Leeds, LS2 9JT, UK.

Notes

The authors declare no competing financial interests.

ACKNOWLEDGEMENT

A.D. gratefully acknowledges the financial support received from the DST Ramanujan fellowship scheme (SB/S2/RJN-119/2015) and UGC start-up grant (F.4-5(244-FRP)/2015/BSR). A.S. would like to gratefully acknowledge the contributions of Stuart Micklethwaite (LEMAS – Leeds Electron Microscopy and Spectroscopy Centre, Faculty of Engineering, University of Leeds) for cryo-SEM of the LC emulsion droplets and would like to thank Dr. Andrea Araiza-Calahorra for the interfacial shear rheology experiments. The Zeiss LSM880 confocal microscope used in this work was funded by the Wellcome Trust multi-user equipment award WT104918MA.

REFERENCES

(1) Lin, I.-H.; Miller, D. S.; Bertics, P. J.; Murphy, C. J.; Pablo, J. J. de; Abbott, N. L. Endotoxin-Induced Structural Transformations in Liquid Crystalline Droplets. *Science* **2011**, *332*, 1297–1300.

(2) Miller, D. S.; Abbott, N. L. Influence of Droplet Size, pH and Ionic Strength on Endotoxin Triggered Ordering Transitions in Liquid Crystalline Droplets. *Soft Matter* **2013**, *9*, 374–382.

(3) Miller, D. S.; Wang, X.; Buchen, J.; Lavrentovich, O. D.; Abbott, N. L. Analysis of the Internal Configurations of Droplets of Liquid Crystal Using Flow Cytometry. *Anal. Chem.* **2013**, *85*, 10296–10303.

(4) Bai, Y.; Abbott, N. L. Recent Advances in Colloidal and Interfacial Phenomena Involving Liquid Crystals. *Langmuir* **2011**, *27*, 5719–5738.

(5) Lowe, A. M.; Abbott, N. L. Liquid Crystalline Materials for Biological Applications. *Chem. Mater.* **2012**, *24*, 746–758.

(6) Tjipto, E.; Cadwell, K. D.; Quinn, J. F.; Johnston, A. P. R.; Abbott, N. L.; Caruso, F. Tailoring the Interfaces between Nematic Liquid Crystal Emulsions and Aqueous Phases via Layer-by-Layer Assembly. *Nano Lett.* **2006**, *6*, 2243–2248.

(7) Gupta, J. K.; Sivakumar, S.; Caruso, F.; Abbott, N. L. Size-Dependent Ordering of Liquid Crystals Observed in Polymeric Capsules with Micrometer and Smaller Diameters. *Angew. Chemie* **2009**, *48*, 1652–1655.

(8) Ramezani-Dakhel, H.; Rahimi, M.; Pendery, J.; Kim, Y.-K.; Thayumanavan, S.; Roux, B.; Abbott, N. L.; Pablo, J. J. de. Amphiphile-Induced Phase Transition of Liquid Crystals at Aqueous Interfaces. *ACS Appl. Mater. Interfaces* **2018**, *10*, 37618–37624.

(9) Brake, J. M.; Daschner, M. K.; Luk, Y.-Y.; Abbott, N. L. Biomolecular Interactions at Phospholipid-Decorated Surfaces of Liquid Crystals. *Science* **2003**, *302*, 2094–2097.

(10) Kirchner, N.; Zedler, L.; Mayerhöfer, T. G.; Mohr, G. J. Functional Liquid Crystal Films Selectively Recognize Amine Vapours and Simultaneously Change Their Colour. *Chem. Commun.* **2006**, 14, 1512–1514.

(11) Aliño, V. J.; Pang, J.; Yang, K.-L. Liquid Crystal Droplets as a Hosting and Sensing Platform for Developing Immunoassays. *Langmuir* **2011**, *27*, 11784–11789.

(12) Aliño, V. J.; Sim, P. H.; Choy, W. T.; Fraser, A.; Yang, K.-L. Detecting Proteins in Microfluidic Channels Decorated with Liquid Crystal Sensing Dots. *Langmuir* **2012**, *28*, 17571–17577.

(13) Aliño, V. J.; Tay, K. X.; Khan, S. A.; Yang, K.-L. Inkjet Printing and Release of Monodisperse Liquid Crystal Droplets from Solid Surfaces. *Langmuir* **2012**, *28*, 14540–14546.

(14) Bi, X.; Lai, S. L.; Yang, K.-L. Liquid Crystal Multiplexed Protease Assays Reporting Enzymatic Activities as Optical Bar Charts. *Anal. Chem.* **2009**, *81*, 5503–5509.

(15) Bera, T.; Fang, J. Optical Detection of Lithocholic Acid with Liquid Crystal Emulsions. *Langmuir* **2013**, *29*, 387–392.

(16) Bera, T.; Fang, J. Polyelectrolyte-Coated Liquid Crystal Droplets for Detecting Charged Macromolecules. *J. Mater. Chem.* **2012**, *22*, 6807–6812.

(17) Sivakumar, S.; Wark, K. L.; Gupta, J. K.; Abbott, N. L.; Caruso, F. Liquid Crystal Emulsions as the Basis of Biological Sensors for the Optical Detection of Bacteria and Viruses. *Adv. Funct. Mater.* **2009**, *19*, 2260–2265.

(18) Kinsinger, M. I.; Buck, M. E.; Abbott, N. L.; Lynn, D. M. Immobilization of Polymer-Decorated Liquid Crystal Droplets on Chemically Tailored Surfaces. *Langmuir* **2010**, *26*, 10234–10242.

(19) Miller, D. S.; Carlton, R. J.; Mushenheim, P. C.; Abbott, N. L. Introduction to Optical Methods for Characterizing Liquid Crystals at Interfaces. *Langmuir* **2013**, *29*, 3154–3169.

(20) Khan, W.; Choi, J. H.; Kim, G. M.; Park, S.-Y. Microfluidic Formation of pH Responsive 5CB Droplets Decorated with PAA-b-LCP. *Lab Chip* **2011**, *11*, 3493–3498.

(21) Kim, J.; Khan, M.; Park, S.-Y. Glucose Sensor Using Liquid Crystal Droplets Made by Microfluidics. *ACS Appl. Mater. Interfaces* **2013**, *5*, 13135–13139.

(22) Chang, C.-Y.; Chen, C.-H. Oligopeptide-Decorated Liquid Crystal Droplets for Detecting Proteases. *Chem. Commun.* **2014**, *50*, 12162–12165.

(23) Yoon, S. H.; Gupta, K. C.; Borah, J. S.; Park, S.-Y.; Kim, Y.-K.; Lee, J.-H.; Kang, I.-K. Folate Ligand Anchored Liquid Crystal Microdroplets Emulsion for *in Vitro* Detection of KB Cancer Cells. *Langmuir* **2014**, *30*, 10668–10677.

(24) Verma, I.; Pani, I.; Sharma, D.; Maity, S.; Pal, S. K. Label-Free Imaging of Fibronectin Adsorption at Poly-(L-Lysine)-Decorated Liquid Crystal Droplets. *J. Phys. Chem. C* **2019**, *123*, 13642–13650.

(25) Verma, I.; Sidiq, S.; Pal, S. K. Poly(L-lysine)-Coated Liquid Crystal Droplets for Sensitive Detection of DNA and Their Applications in Controlled Release of Drug Molecules. *ACS Omega* **2017**, *2*, 7936–7945.

(26) Sidiq, S.; Prasad, G. V. R. K.; Mukhopadhaya, A.; Pal, S. K. Poly(L-lysine)-Coated Liquid Crystal Droplets for Cell-Based Sensing Applications. *J. Phys. Chem. B* **2017**, *121*, 4247–4256.

(27) Upadhyay, A. P.; Sadhukhan, P.; Roy, S.; Pala, R. G. S.; Sivakumar, S. Brownian Motion Retarded Polymer-Encapsulated Liquid Crystal Droplets Anchored Over a Patterned Substrate via Click Chemistry. *RSC Adv.* **2014**, *4*, 27135–27139.

(28) Guo, X.; Manna, U.; Abbott, N. L.; Lynn, D. M. Covalent Immobilization of Caged Liquid Crystal Microdroplets on Surfaces. *ACS Appl. Mater. Interfaces* **2015**, *7*, 26892–26903.

(29) Deng, J.; Liang, W.; Fang, J. Liquid Crystal Droplet-Embedded Biopolymer Hydrogel Sheets for Biosensor Applications. *ACS Appl. Mater. Interfaces* **2016**, *8*, 3928–3932.

(30) Hussain, A.; Semeano, A. T. S.; Palma, S. I. C. J.; Pina, A. S.; Almeida, J.; Medrado, B. F.; Pádua, A. C. C. S.; Carvalho, A. L.; Dionísio, M.; Li, R. W. C.; Gamboa, H.; Ulijn, R. V.; Gruber, J.; Roque, A. C. A. Tunable Gas Sensing Gels by Cooperative Assembly. *Adv. Funct. Mater.* **2017**, *27*, 1-9.

(31) Binks, B. P. Particles as Surfactants-Similarities and Differences. *Curr. Opin. Colloid Interface Sci.* **2002**, *7*, 21–41.

(32) Dan, A.; Agnihotri, P.; Brugnoni, M.; Siemes, E.; Woll, D.; Crassous, J. J.; Richtering, W. Microgel-Stabilized Liquid Crystal Emulsions Enable an Analyte-Induced Ordering Transition. *Chem. Commun.* **2019**, *55*, 7255–7258.

(33) Schmitt, C.; Moitzi, C.; Bovay, C.; Rouvet, M.; Bovetto, L.; Donato, L.; Leser, M. E.; Schurtenberger, P.; Stradner, A. Internal Structure and Colloidal Behaviour of Covalent Whey Protein Microgels Obtained by Heat Treatment. *Soft Matter* **2010**, *6*, 4876–4884.

(34) Sarkar, A.; Kanti, F.; Gulotta, A.; Murray, B. S.; Zhang, S. Aqueous Lubrication, Structure and Rheological Properties of Whey Protein Microgel Particles. *Langmuir* **2017**, *33*, 14699–14708.

(35) Sarkar, A.; Murray, B.; Holmes, M.; Ettelaie, R.; Abdalla, A.; Yang, X. *In vitro* Digestion of Pickering Emulsions Stabilized by Soft Whey Protein Microgel Particles: Influence of Thermal Treatment. *Soft Matter* **2016**, *12*, 3558–3569.

(36) Araiza-Calahorra, A.; Sarkar, A. Pickering Emulsion Stabilized by Protein Nanogel Particles for Delivery of Curcumin : Effects of pH and Ionic Strength on Curcumin Retention. *Food Struct.* **2019**, *21*, 1–12.

(37) Andablo-Reyes, E.; Yerani, D.; Fu, M.; Liamas, E.; Connell, S.; Torres, O.; Sarkar, A. Microgels as Viscosity Modifiers Influence Lubrication Performance of Continuum. *Soft Matter* **2019**, *15*, 9614–9624.

(38) Torres, O.; Murray, B. S.; Sarkar, A. Overcoming *In vitro* Gastric Destabilisation of Emulsion Droplets Using Emulsion Microgel Particles for Targeted Intestinal Release of Fatty Acids. *Food Hydrocoll.* **2019**, *89*, 523–533.

(39) Cheng, L.; Ye, A.; Hemar, Y.; Gilbert, E. P.; Campo, L. de; Whitten, A. E.; Singh, H. Interfacial Structures of Droplet-Stabilized Emulsions Formed with Whey Protein Microgel Particles as Revealed by Small- and Ultra-Small-Angle Neutron Scattering. *Langmuir* **2019**, *35*, 12017–12027.

(40) Destribats, M.; Rouvet, M.; Gehin-Delval, C.; Schmidtt, C.; Binks, B. P. Emulsions Stabilised by Whey Protein Microgel Particles: Towards Food-Grade Pickering Emulsions. *Soft Matter* **2014**, *10*, 6941–6954.

(41) Sarkar, A.; Zhang, S.; Holmes, M.; Ettelaie, R. Colloidal Aspects of Digestion of Pickering Emulsions: Experiments and Theoretical Models of Lipid Digestion Kinetics. *Adv. Colloid Interface Sci.* **2019**, *263*, 195–211.

(42) Dickinson, E. Biopolymer-Based Particles as Stabilizing Agents for Emulsions and Foams. *Food Hydrocoll.* **2017**, *68*, 219–231.

(43) Style, R. W.; Isa, L.; Dufresne, E. R. Adsorption of Soft Particles at Fluid Interfaces. *Soft Matter* **2015,** *11*, 7412-7419.

(44) Murray, B. S.; Phisarnchananan, N. Whey Protein Microgel Particles as Stabilizers of Waxy Corn Starch + Locust Bean Gum Water-in-Water Emulsions. *Food Hydrocoll.* **2016**, *56*, 161–169.

(45) Arditty, S.; Whitby, C. P.; Binks, B. P.; Schmitt, V.; Leal-Calderon, F. Some General Features of Limited Coalescence in Solid-Stabilized Emulsions. *Eur. Phys. J. E* **2003**, *11*, 273–281.

(46) O'Brien, R. W. Electro-Acoustic Effects in a Dilute Suspension of Spherical Particles. *J. Fluid Mech.* **1988**, *190*, 71–86.

(47) Sarkar, A.; Juan, J.-M.; Kolodziejczyk, E.; Acquistapace, S.; Donato-Capel, L.; Wooster,

T. J. Impact of Protein Gel Porosity on the Digestion of Lipid Emulsions. *J. Agric. Food Chem.* **2015**, *63*, 8829–8837.

(48) Phan-Xuan, T.; Durand, D.; Nicolai, T.; Donato, L.; Schmitt, C.; Bovetto, L. On the Crucial Importance of the pH for the Formation and Self-Stabilization of Protein Microgels and Strands. *Langmuir* **2011**, *27*, 15092–15101.

(49) Tcholakova, S.; Denkov, N. D.; Lips, A. Comparison of Solid Particles, Globular Proteins and Surfactants as Emulsifier. *Phys. Chem. Chem. Phys.* **2008**, *9*, 1608–1627.

(50) Simon, K. A.; Sejwal, P.; Gerecht, R. B.; Luk, Y.-Y. Water-in-Water Emulsions Stabilized by Non-Amphiphilic Interactions: Polymer-Dispersed Lyotropic Liquid Crystals. *Langmuir* **2007**, *23*, 1453–1458.

(51) Brugger, B.; Vermant, J.; Richtering, W. Interfacial Layers of Stimuli-Responsive Poly-(N-isopropylacrylamide-co-methacrylicacid) (PNIPAM-co-MAA) Microgels Characterized by Interfacial Rheology and Compression Isotherms. *Phys. Chem. Chem. Phys.* **2010**, *12*, 14573–14578.

(52) Lockwood, N. A.; Cadwell, K. D.; Caruso, F.; Abbott, N. L. Formation of Polyelectrolyte Multilayer Films at Interfaces Between Thermotropic Liquid Crystals and Aqueous Phases. *Adv. Mater.* **2006**, *18*, 850–854.

(53) Bhuyan, A. K. On the Mechanism of SDS-Induced Protein Denaturation. *Biopolymers* **2010**, *93*, 186–199.

(54) Hsu, C.-T.; Shao, M.-J.; Lin, S.-Y. Adsorption Kinetics of $C_{12}E_4$ at the Air-Water Interface: Adsorption onto a Fresh Interface. *Langmuir* **2000**, *16*, 3187–3194.

Supplementary File

Protein Microgel-Stabilized Pickering Liquid Crystal Emulsions Undergo Analyte-Triggered Configurational Transition

Abhijit Dan,*[†] Shikha Aery,[†] Shuning Zhang,[‡] Daniel Baker,[$] Helen F. Gleeson,[$] Anwesha Sarkar*[‡]

[†]Department of Chemistry and Centre for Advanced Studies in Chemistry, Panjab University − Chandigarh, Sector 14, Chandigarh, 160014, India

[‡]Food Colloids and Bioprocessing Group, School of Food Science and Nutrition, University of Leeds, LS2 9JT, UK.

[$]Soft Matter Physics Group, School of Physics and Astronomy, University of Leeds, LS2 9JT, UK.

Email: abhijit@pu.ac.in (A.D.); a.sarkar@leeds.ac.uk (A.S.)

867

868

869

870

871 **Table S1. ζ-potentials of WPM-stabilized Pickering LC-in-emulsions dispersed in 5 mM SDS or**

872 **DTAB solutions***

[WPM] (wt %)	ζ-Potential (mV)	
	5 mM SDS solution	5 mM DTAB solution
0.005	- 62.1 ± 1.6 [a]	12.9 ± 3.8 [b]
0.01	- 63.3 ± 4.3 [a]	15.7 ± 2.5 [b]
0.05	- 65.6 ± 4.7 [a]	9.4 ± 3.2 [b]
0.1	- 66.1 ± 3.9 [a]	10.4 ± 3.7 [b]
1	- 61.7 ± 3.6 [a]	13.0 ± 4.3 [b]

873 *The values represent means ± standard deviations of at least three independent experiments on triplicate
874 samples (n = 3 × 3). Samples with the same letter do not differ significantly ($p > 0.05$) according to Tukey's
875 test.

876

877

878

879

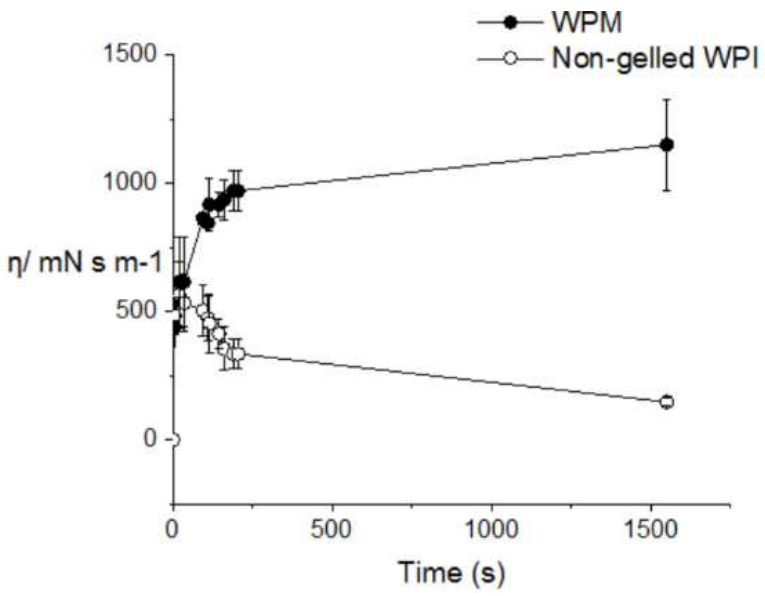

Figure S1. Interfacial shear viscosities (η_i / mN s m^{-1}) at *n*-tetradecane-water interface in presence of non-microgelled whey protein isolate (WPI) and whey protein microgel particles (WPM) at pH 7. The data points represent mean ± SD of at least three independent experiments on triplicate samples (n = 3 × 3).

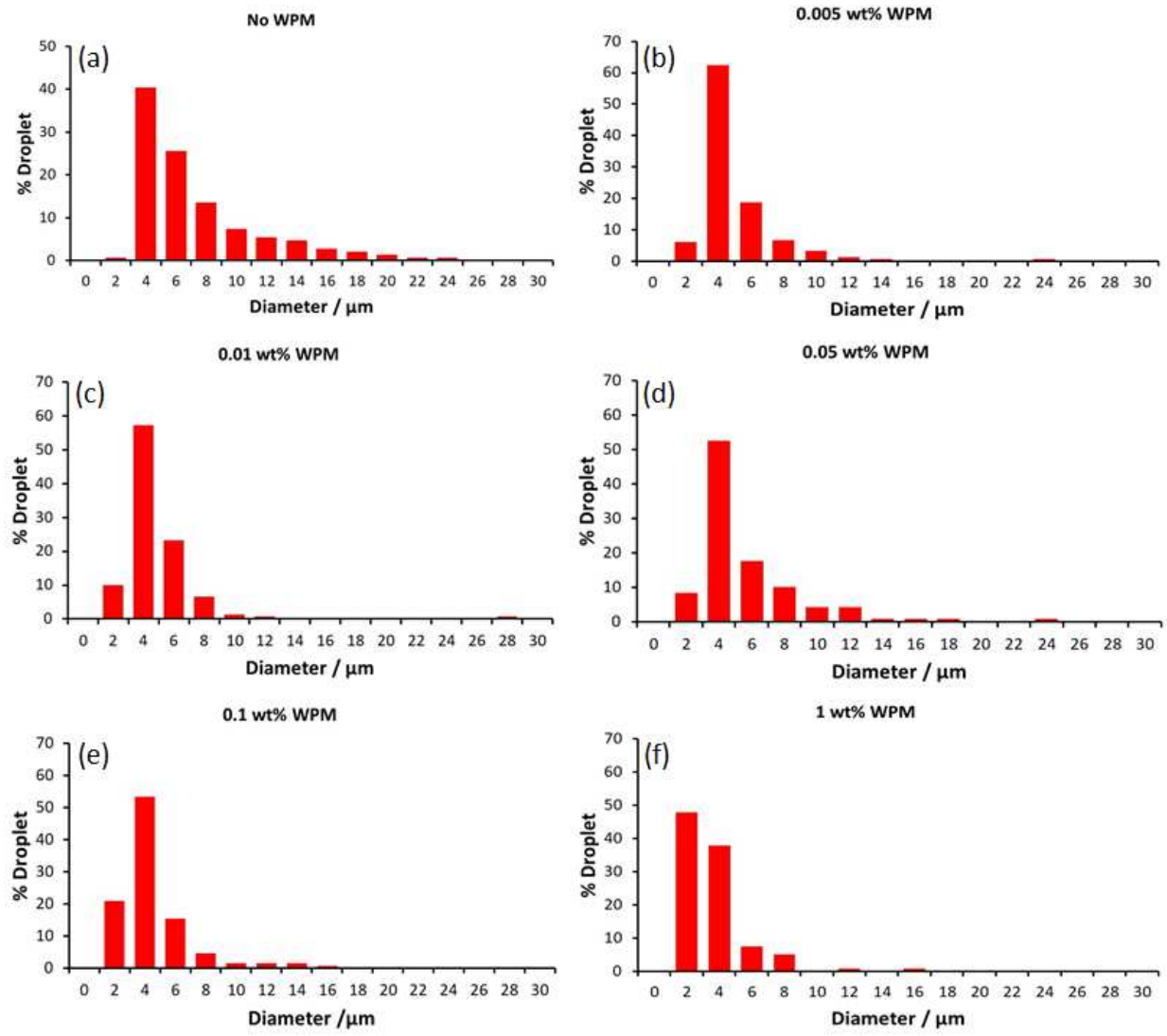

891

892 **Figure S2.** Size distribution of freshly prepared LC-in-water emulsion droplets stabilized by (a) 0, (b)
893 0.005, (c) 0.01, (d) 0.05, (e) 0.1 and (f) 1 wt % WPM particles obtained from optical microscopy (bright
894 field) measurements, calculated using Image J software.

895

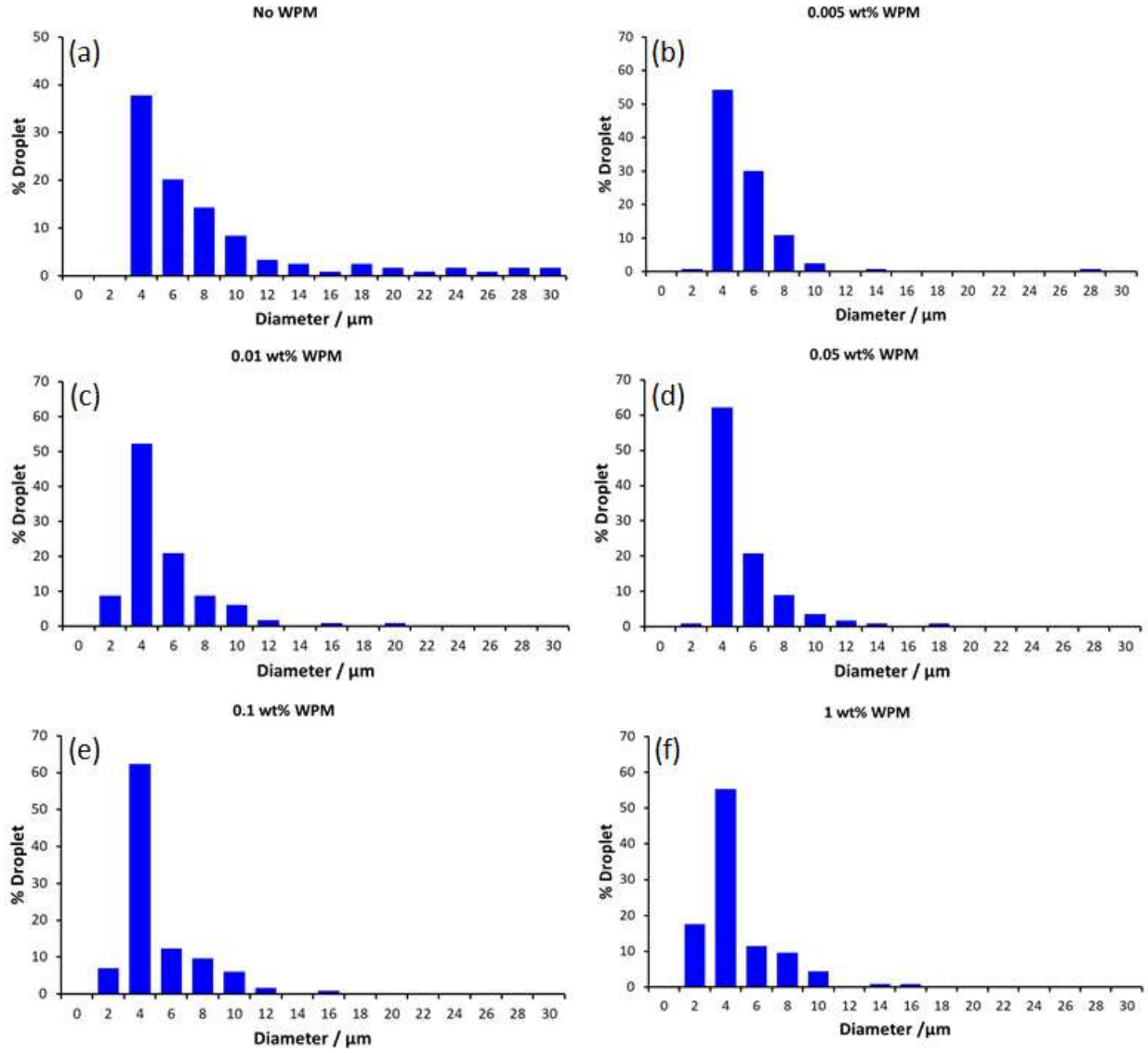

Figure S3. Size distribution of LC-in-water emulsion droplets stabilized by (a) 0, (b) 0.005, (c) 0.01, (d) 0.05, (e) 0.1 and (f) 1 wt % WPM particles obtained from optical microscopy (bright field) measurements after 14 days of storage post-preparation, calculated using Image J software.

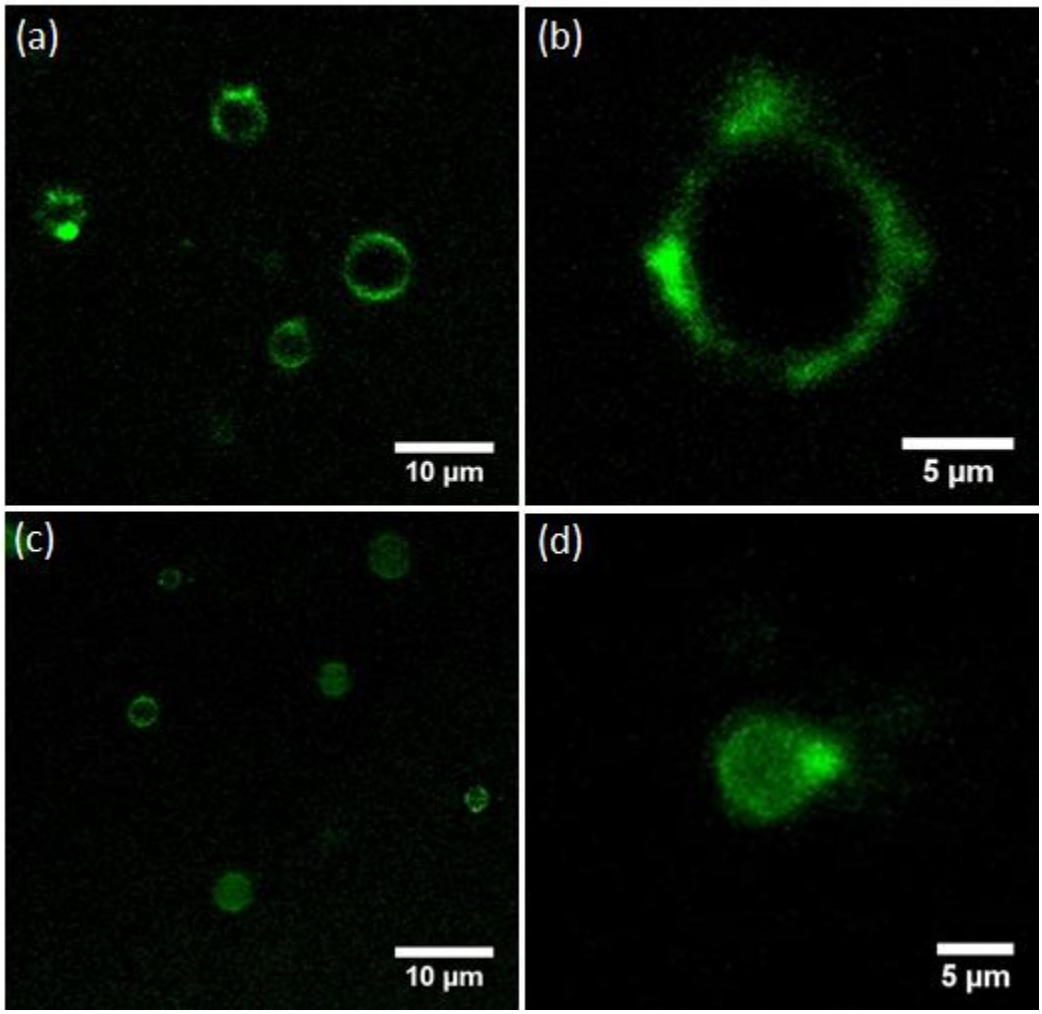

Figure S4. Confocal microscopy images of LC-in-water emulsion droplets stabilized by (a,b) 0.005 and (c,d) 1 wt % WPM at different magnifications measured after 14 days of storage post-preparation with (a,c) showing arrays of LC droplets dispersed in aqueous medium and (b,d) showing single droplet covered by WPM.

912

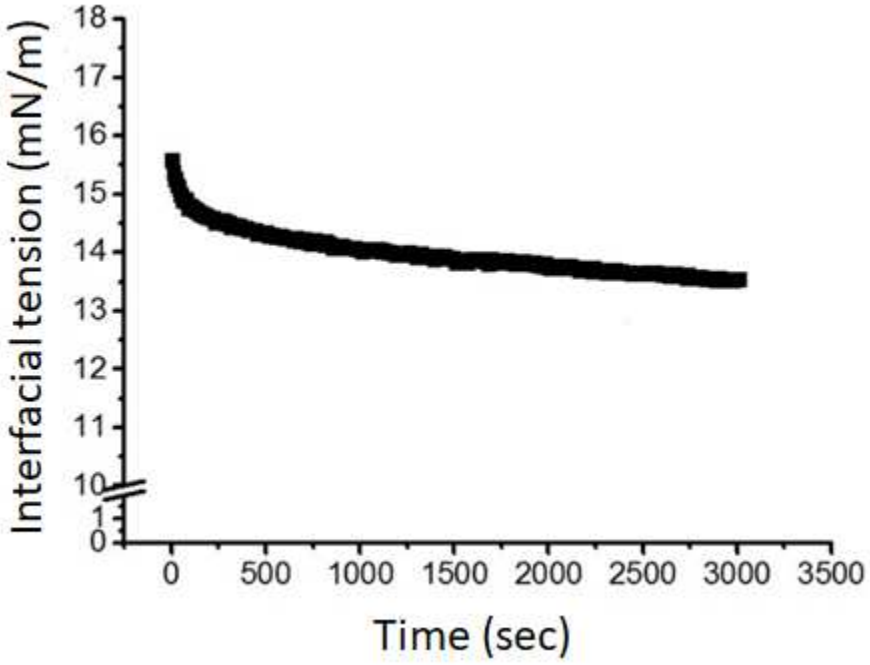

Figure S5. Interfacial tension (mN m^{-1}) between MilliQ water and *n*-tetradecane in presence of whey protein microgel particles (WPM) at pH 7. The data points represent mean ± SD of at least three independent experiments on triplicate samples (n = 3 × 3).

927

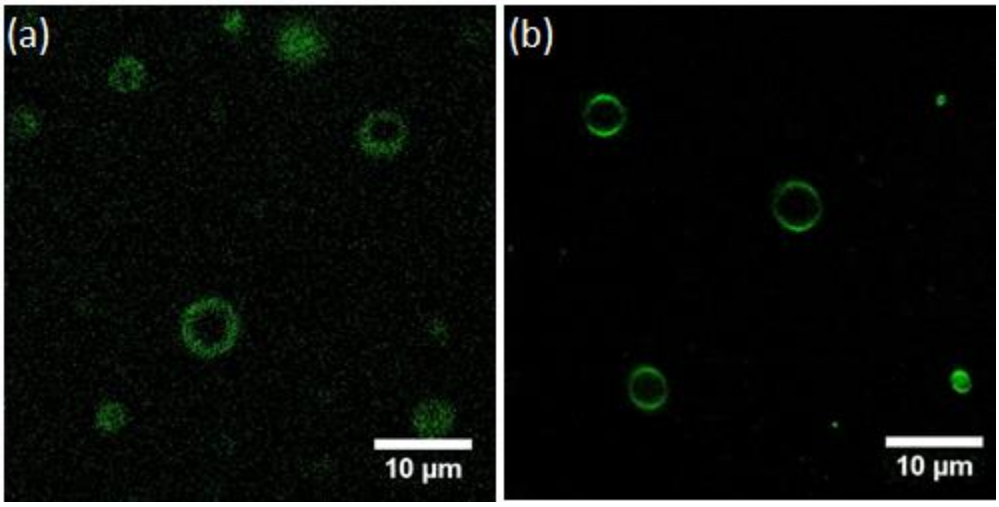

928

929 **Figure S6.** Confocal microscopy images of LC-in-water emulsion droplets stabilized by 0.01 wt% WPM

930 dispersed in (a) SDS-free aqueous medium and (b) 5 mM SDS solution, respectively.

931

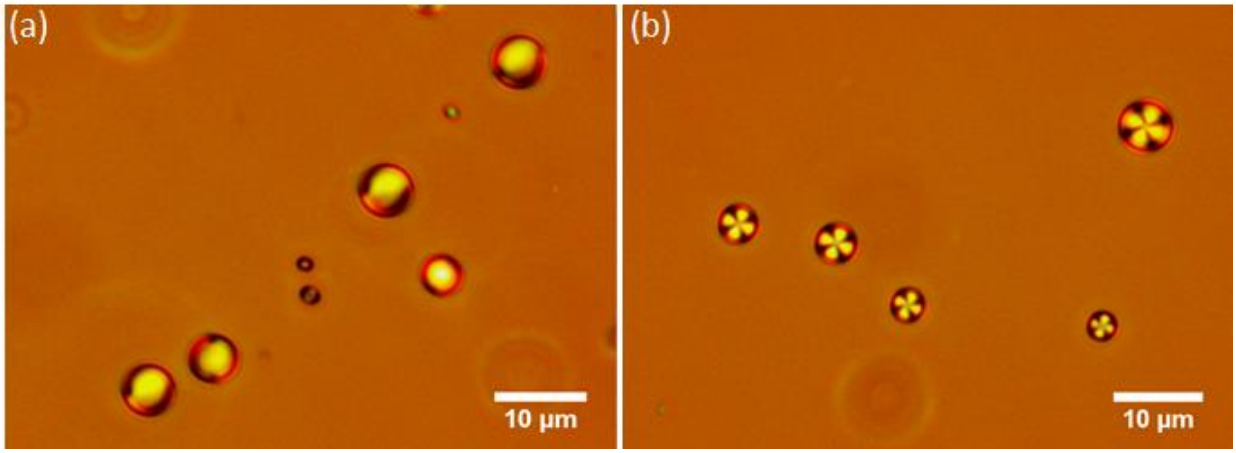

Figure S7. Polarized light microscopy images of WPM-stabilized Pickering LC droplets deposited on the bottom surface from the (a) SDS-free aqueous medium with bipolar signature and (b) 5 mM SDS solution with radial signature, respectively.

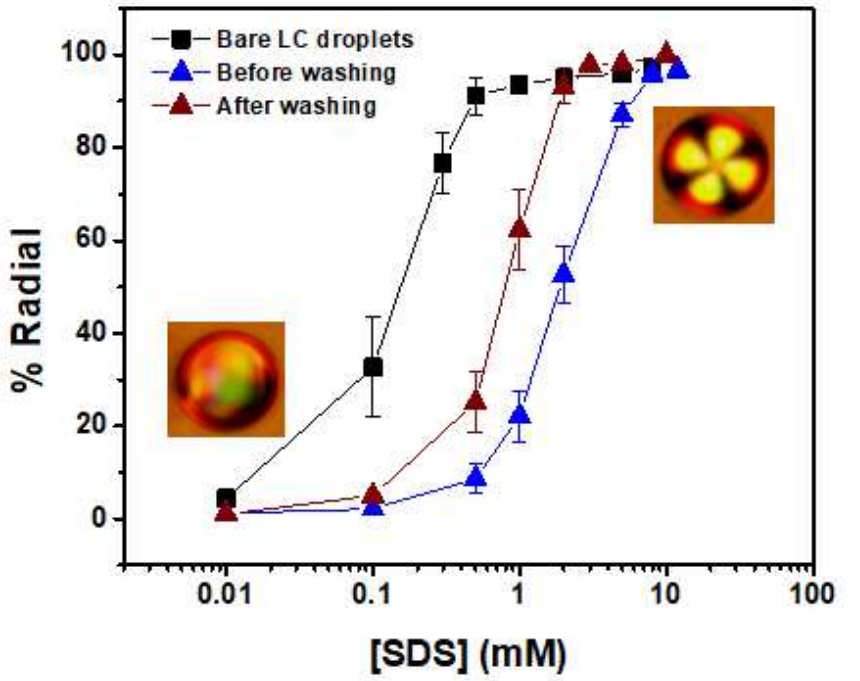

Figure S8. Comparison of LC response to SDS for WPM-stabilized Pickering LC droplets (0.01 wt % WPM) before and after removal of excess unadsorbed WPM from the aqueous medium, and further that obtained with bare LC droplets (no WPM coating). The measurements were taken at a fixed droplet concentration of 2×10^6 mL^{-1}. The data points represent means ± standard deviations of at least three independent experiments on triplicate samples ($n = 3 \times 3$).

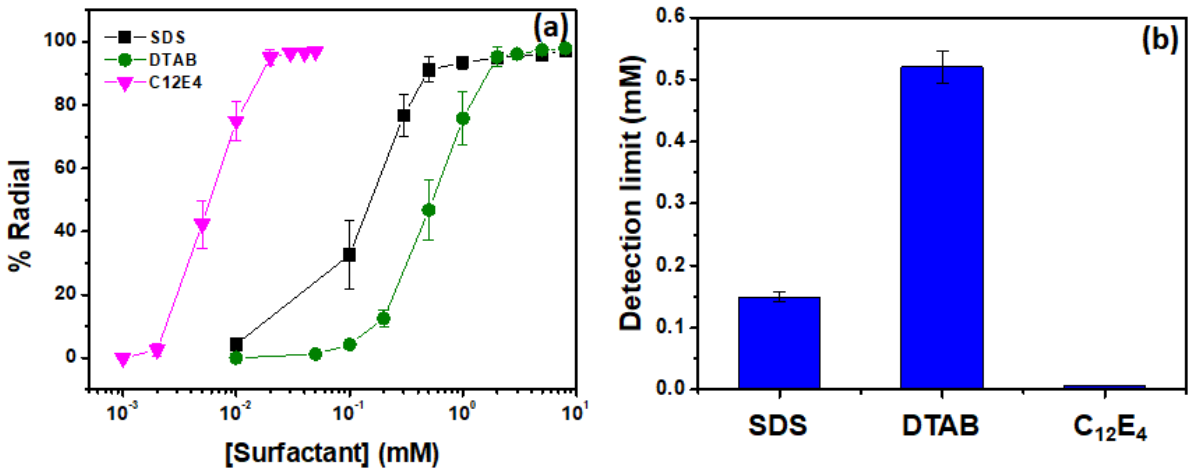

946

947 **Figure S9.** (a) Dose-response curves of bare LC droplets for SDS, DTAB and $C_{12}E_4$ measured at a fixed

948 droplet concentration of 2×10^6 mL^{-1} and (b) detection limit of bare LC droplets for SDS, DTAB and $C_{12}E_4$.

949 The data points represent means ± standard deviations of at least three independent experiments on triplicate

950 samples (n = 3 × 3).

951